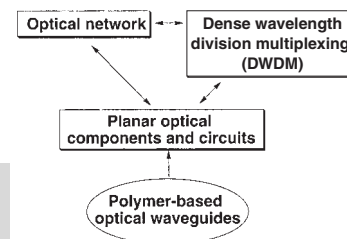


# Polymer-Based Optical Waveguides: Materials, Processing, and Devices\*\*

By Hong Ma, Alex K.-Y. Jen,\* and Larry R. Dalton



*Polymer optical waveguide devices will play a key role in several rapidly developing areas of broadband communications, such as optical networking, metropolitan/access communications, and computing systems due to their easier processibility and integration over inorganic counterparts. The combined advantages also makes them an ideal integration platform where foreign material systems such as YIG (yttrium iron garnet) and lithium niobate, and semiconductor devices such as lasers, detectors, amplifiers, and logic circuits can be inserted into an etched groove in a planar light-wave circuit to enable full amplifier modules or optical add/drop multiplexers on a single substrate. Moreover, the combination of flexibility and toughness in optical polymers makes it suitable for vertical integration to realize 3D and even all-polymer integrated optics. In this review, a survey of suitable optical polymer systems, their processing techniques, and the integrated optical waveguide components and circuits derived from these materials is summarized. The first part is focused on discussing the characteristics of several important classes of optical polymers, such as their refractive index, optical loss, processibility/mechanical properties, and environmental performance. Then, the emphasis is placed on the discussion of several novel passive and active (electro-optic and thermo-optic) polymer systems and versatile processing techniques commonly used for fabricating component devices, such as photoresist-based patterning, direct lithographic patterning, and soft lithography. At the end, a series of compelling polymer optical waveguide devices including optical interconnects, directional couplers, array waveguide grating (AWG) multi/demultiplexers, switches, tunable filters, variable optical attenuators (VOAs), and amplifiers are reviewed. Several integrated planar lightwave circuits, such as tunable optical add/drop multiplexers (OADMs), photonic crystal superprism waveguides, digital optical switches (DOSs) integrated with VOAs, traveling-wave heterojunction phototransistors, and three-dimensionally (3D) integrated optical devices are also highlighted.*

## 1. Introduction

Over the last two decades, advances in electronics have revolutionized the speed with which we perform computing and communications of all kinds. Three key technologies were

combined to create a platform that enabled the electronic revolution: semiconductor materials, automated microfabrication of integrated electronic circuits, and integrated electronic circuit design. As a result, the mass manufacturing of low-cost integrated circuits has become possible. However, currently, bandwidth demand is outgrowing the performance of electronics in many applications. Signal propagation and switching speeds in the electronic domain are inherently limited. One area where these limitations are clearly seen is in telecommunications, where bandwidth expansion is desperately needed. To overcome these barriers, we must enter a new computing and communications revolution based on photonics which is known to outperform electronics in many areas. Photonics applications have an extremely large information capacity (very broad bandwidth) and very low transmission losses and heat generation, are immune to crosstalk and electromagnetic interference, and are lightweight and smaller in size compared to electronics. Photons also do not interact linearly when multiple wavelengths propagate in an optical medium, and thus

[\*] Prof. A. K.-Y. Jen, Dr. H. Ma  
Department of Materials Science & Engineering, Box 352120  
University of Washington  
Seattle, WA 98195-2120 (USA)  
E-mail: ajen@u.washington.edu  
Prof. L. R. Dalton  
Department of Chemistry, Box 351700  
University of Washington  
Seattle, WA 98195-1700 (USA)

[\*\*] Financial support from the National Science Foundation (NSF-NIRT), the Boeing-Johnson Foundation, and the Air Force Office of Scientific Research (AFOSR) through the MURI Center (Polymeric Smart Skins) is acknowledged. We appreciate Drs. A. Donval, L. Eldada, M. Hikita, N. Keil, R. A. Norwood, R. Hauffe, J. Kenney, and Profs. Y. Ohmori, K. Petermann, W. H. Steier, and H. R. Fetterman for their kindness in providing some of the figures cited in this review and for very helpful discussions.

allow parallel processing of different wavelengths. Moreover, photonics plays a crucial and complementary role to electronics in many application domains. Examples of successful uses of photonics can be found in broadband communications, high-capacity information storage, and large-screen and portable information displays.<sup>[1]</sup>

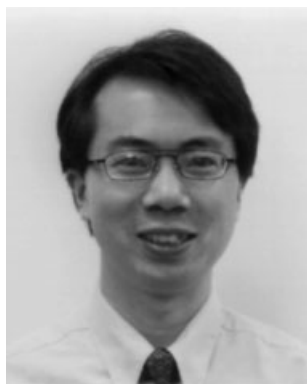
Broadband communications (telecom and datacom) can be realized through either free-space optics or guided-wave optics. Free-space optics (FSO), also called free-space photonics (FSP), refers to the transmission of modulated visible or infrared (IR) beams through the atmosphere to obtain broadband communications. As a matter of fact, FSO systems can function over distances of several kilometers as long as there is a clear line of sight between the source and the destination. Nevertheless, there are limitations to FSO due to rain, dust, snow, fog, or smog, which can invariably block the transmis-

sion path. Guided-wave optics, however, depends on the phenomenon of total internal reflection (TIR), which can confine light in the optical waveguide, a material surrounded by other materials with lower refractive indices (Fig. 1a). Optical waveguides may be thin-film deposits used in integrated optical circuits or a filament of dielectric material usually circular in the cross section used in fiber optics. Depending on the various possible patterns of propagating or standing electromagnetic fields, there are single-mode and multi-mode optical waveguides. Each mode is characterized by its frequency, effective refractive index, polarization, power distribution, electric field strength, and magnetic field strength.<sup>[2]</sup>

Optical waveguiding was first referred to as "light piping" in 1880 by Wheeler; this is what we now know as fiber optics because he transmitted light through a glass pipe medium. However, with the invention of lasers and the development of



*Alex Jen received his Ph.D. degree in Organic Chemistry from the University of Pennsylvania in 1984 under the tutelage of Professor Michael Cava. He started his career as a Research Chemist at Allied-Signal Inc., (1984–1988) where he was responsible for the discovery of several classes of processible and thermally stable conducting polymers for opto-electronic applications. In 1988, he joined Enichem America Inc. as a Principal Scientist and established the nonlinear optical (NLO) materials program in the company. He moved to ROI Technology in 1995, where he was Vice President of materials. In 1997, he joined Northeastern University as an Associate Professor at the Department of Chemistry, moving to the University of Washington at Seattle in 1999 as the Boeing-Johnson Chair Professor. His research interests are focused on the design, synthesis, and characterization of novel conjugated materials, NLO dendrimers, highly fluorinated polymers, self-assembled monolayers and block copolymers, and hybrid materials. He has co-authored more than 220 papers and 25 patents on topics related to materials chemistry and devices.*



*Hong Ma received his Ph.D. degree in Organic Chemistry in 1997 from Nankai University, P. R. China under the tutelage of Professors Jiben Meng and Yuquan Shen. From 1997 to 2001 he worked as a postdoctoral researcher in Prof. Alex K.-Y. Jen's group at the University of Washington and Northeastern University. He is currently a Research Scientist in the Department of Materials Science and Engineering, University of Washington, where his research is concentrated on the design, synthesis, and characterization of organic functional molecules, polymers, and dendrimers for photonic applications and molecular electronics.*



*Larry Dalton obtained his Ph.D. in chemistry from Harvard University in 1971. He received an Alfred P. Sloan Fellowship (1974–77), a Camille and Henry Dreyfus Teacher-Scholar Award (1975–77), and a Development Award (1976–81) and has held several appointments at different universities and companies since then. He was the Director of the DoD MURI Center on Materials and Processing at the Nanometer Scale between 1996 and 2001 and currently holds multiple faculty appointments at the University of Washington (Seattle) and University of Southern California (Los Angeles). He has received several awards, including a Distinguished Alumni Award of Michigan State University (2000), the 2003 Chemistry of Materials Award of the American Chemical Society, and the 1996 Richard C. Tolman Medal of the American Chemical Society. He has authored over 400 research papers and texts on topics ranging from materials science to devices.*

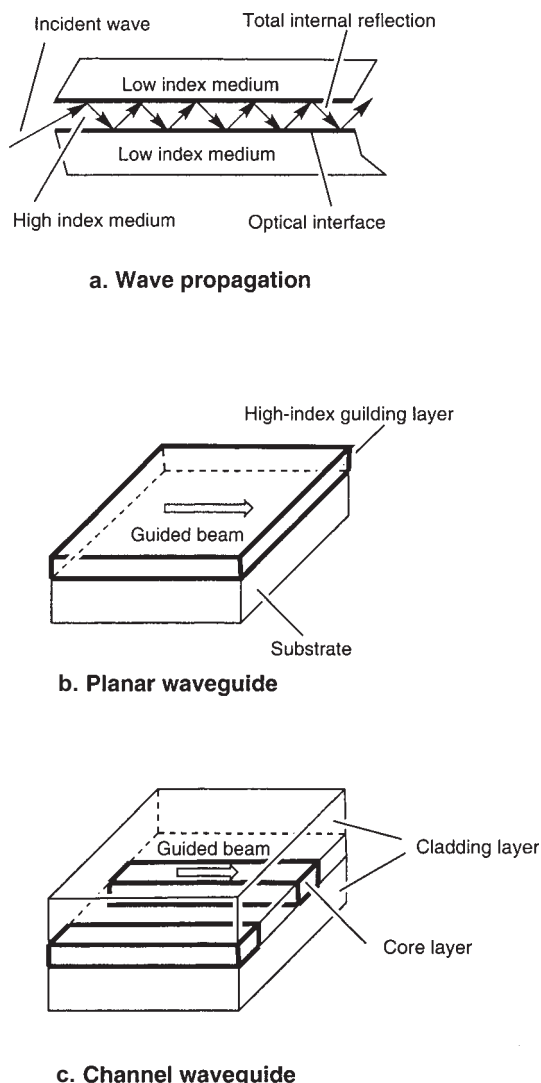


Fig. 1. The principle of optical waveguides and structures of planar and channel waveguides.

coherent optics, the need for a long-distance transmission medium (optical fiber) and guiding structure with which to build optical components and connect them into optical circuits arose. These optical waveguides allow the fabrication of planar components and their integration into planar optical circuits. This configuration proved efficient and showed many advantages in electronic circuits at all frequencies up to the microwave range. To achieve this goal, planar fabrication and integration require planar optical waveguides in the form of films and strips. Rectangular dielectric waveguides were first studied theoretically by Schlosser in 1964, and film waveguides as well as other planar components and circuitry for applications in the infrared range were constructed by Anderson in 1965. These and other early efforts in the development of planar optical waveguides and circuits received additional support and stimulus when Miller surveyed the advantages and possibilities of this technology and coined the term “integrated optics” for it in 1969. Since then, not only has the theo-

ry of wave propagation, excitation, and the conjugation of optical films and strips been advanced to encompass all aspects in the analysis and design of these guiding structures, but also precise and reliable technologies have been developed to fabricate planar optical waveguides and integrated optical circuits.<sup>[3]</sup>

Planar waveguide integrated optics involves the manipulation of sheet beams that are confined in one dimension. These can propagate in any direction parallel to the surface of a high-index guiding layer. By loading a thin film with a higher refractive index than the substrate, the light can be trapped inside this film and waveguides are produced. Waveguides where the refractive index changes in discrete steps are called step-index (SI) optical waveguides, whereas those with a gradual refractive-index change are called graded-index (GI) optical waveguides. Figure 1b shows a typical three-layer SI planar waveguide. It can be formed by depositing a thin layer of material with higher refractive index on a substrate with a lower index. The third layer is usually air, or an additional low-index cover layer that can be used. An optical waveguide that is uniform in the direction of propagation is the most basic type of waveguide, but this alone is not sufficient for construction of an optical integrated circuit. In reality, an appropriate combination of various types of optical waveguides is placed on a substrate to construct an optical circuit with desired features. A 2D optical waveguide can trap light in the direction of the film thickness ( $y$  direction) but can allow light to spread in the horizontal direction ( $x$  direction). To facilitate the construction of optical integrated circuits, various types of 3D optical waveguides, or optical channel waveguides (Fig. 1c), which trap the light in both  $x$  and  $y$  directions, have been manufactured. Although waveguides come in various forms and with a variety of functions, such as crossed waveguides, which are used for combining, the fact remains that optical waveguides that are uniform in the direction of propagation are the most basic form.<sup>[4]</sup> Therefore, the following discussion will be limited to optical waveguides in which materials constants, such as structure and refractive index, do not change in the direction of propagation.

Although it seems that optical waveguides are more related to short-distance integrated optics, optical networking *does* mark a fundamental shift in the architecture of fiber communications. Early fiber optic systems were simple long-distance transmission pipelines, carrying signals from point to point. Optical networks aim to organize and process signals in optical form as well as transmit them optically, expanding the realm of light. The ultimate goal is the all-optical network, in which signals stay in optical form throughout the network. In particular, the rapid and global spread of multimedia services including telephone, cable TV, digital video, data and internet capabilities has accelerated the growth in optical communications networks. The most dramatic changes in telecommunications have taken place in the last several years with the advent of optical dense wavelength division multiplexing (DWDM) in the quest for virtually unlimited bandwidth capacity by using the existing optical fiber infrastructure. The huge suc-

cess of DWDM has encouraged telecom equipment vendors to boost network capacity even further by introducing systems that exploit yet more DWDM channels. DWDM has become the leading enabler for an all-optical network. The continuing development of fiber-based communications networks to accommodate future demands will eventually depend on the availability of cheap, reliable, and robust integrated optical waveguide devices for routing, switching, and detection.<sup>[5]</sup>

In addition, broadband communications are also being applied to ever-shortening distances, penetrating from metro-area to access and intra-computer interconnect networks. The current generation of computers is limited by the speed at which information can be transmitted between such electronic components as processors and memory chips. Under these conditions, bus traffic increases as the computing power of the microprocessor increases. Therefore, the limited bus bandwidth constitutes a major bottleneck to efficient communications at the board-to-board data interface. The development of optical interconnects that would replace the conventional passive backplane is desirable in order to achieve higher data throughput.<sup>[6]</sup>

As a result, the further success of broadband communications in optical networking, metro/access communications and computing will rely on the advancement of optical interconnects, optical components, such as splitters, combiners, multiplexers (mux), and demultiplexers (demux), optical switches/modulators, tunable filters, variable optical attenuators, amplifiers, and integrated optical circuits that are based on optical waveguides. While the basic technologies for the design and production of many integrated optical waveguide devices are now in place, there is no clear winner yet in the area of materials<sup>[7]</sup> (Table 1). Today, glass optical fibers are routinely used for high-speed data transfer. Although these fibers provide a convenient means for carrying optical information over

cially at the sales volumes presently experienced for optical components. By using manufacturing techniques closely related to those employed for silicon-integrated circuits, excellent optical components have already been demonstrated using silica-based planar lightwave circuits (PLCs). NTT pioneered the development of silica-based PLCs in 1980; however, it took them almost 15 years to introduce their first commercial product. Currently, optical switches and arrayed-waveguide gratings (AWGs) for multiplexing and de-multiplexing multiple wavelengths in a DWDM system are the predominant applications of silica-based PLC technology.<sup>[8]</sup> The cost issue, the high switching power needed in silica-based switching devices, the low wavelength tuning range, and the temperature dependence of the central wavelength of silica-based AWGs, however, are major problems with this technology. Among the candidate material systems, high expectations have been placed on polymers as the materials choice for highly integrated optical components and circuits.<sup>[9]</sup> State-of-the-art optical polymers are particularly attractive in integrated optical waveguide devices because they offer rapid processibility, cost-effectiveness, high yields, high performance, such as lower optical loss and smaller birefringence compared to silica, power-efficient thermal actuation due to a larger thermo-optic coefficient than in silica, and compactness owing to a large refractive index contrast. Furthermore, polymers provide an ideal platform for the incorporation of more complex material functionalities through selective doping or reaction, thereby enabling amplification and electro-optic effects to be achieved, once the passive optical polymer technology is established. In this article, suitable optical polymers, their processing techniques, and the resulting integrated optical waveguide components and circuits are reviewed.

## 2. Materials

### 2.1. Characteristics of Optical Polymers

#### 2.1.1. Refractive Index

Based on the device design and waveguide geometry, the polymer used as the core material must have a refractive index higher than that of the cladding polymer. The appropriate index difference between core and cladding for either a single-mode or a multi-mode waveguide is strongly dependent on the dimension of the waveguide and the wavelength of the light source.

**Polarizability, Packing Density, and Wavelength Dependence:** The refractive index of a material is related to the free volume (packing density), polarizability of the material, and the difference between the used optical wavelength and the maximum absorption wavelength of the material.<sup>[10]</sup> Usually, dense packing or large polarizability results in an increase in refractive index. Three types of polarizability (electronic, atomic, and dipole orientation) contribute to the total polarization of a material. Electronic polarization is the slight

Table 1. Integrated optics market by material type.

	2001 (US\$ millions)	2005 (US\$ millions)
Silicon	0.4	42.9
Silica on silicon	1.5	282.4
GaAs	2.7	443.7
Indium phosphide	3.0	1 093.5
Lithium niobate	4.0	356.8
Polymer	0.6	207.0
Other	1.1	199.0
TOTAL	13.4	2 625.3

long distances, they are inconvenient for complex high-density circuitry. In addition to being fragile and vibration sensitive, glass fiber devices are difficult to fabricate—especially when they have a high port count—and as a result are quite expensive. InP-based quaternary semiconductor materials are widely employed for waveguide devices, due mainly to their potential for integration with active devices such as lasers and photodetectors operating at around 1550 nm. However, semiconductor processing remains complex and expensive, espe-

skewing of the equilibrium electron distribution relative to the positive nuclei to which it is associated. Since only the movement of electrons is involved, this process can occur very rapidly and typically has a time constant of  $10^{-15}$  s. The atomic polarization results from rearrangement of nuclei in response to an electric field. The positive nuclei are attracted to the negative pole of the applied field. However, the movement of heavy nuclei is more difficult to initiate opposite to that of electrons. As a result, it cannot follow an oscillating field at as high a frequency as the electron response. Dipole orientation polarization results from the redistribution of charge when a group of atoms with a net permanent dipole moment reorients itself in space in response to an electric field. Since large group masses must reorient, this process is usually slower than either electronic or atomic polarization and even in the gas phase will have time constants on the order of  $10^{-9}$  s due to the larger inertia that must be overcome to reverse the direction of movement in each cycle of electric field oscillation. In the liquid or solid phases, large intermolecular forces must be overcome, which slows the process further and decreases the polarization possible under all but static conditions. The dipole orientation polarization is often the dominant mode of polarization contributing to the refractive index in polar liquids and gases. In solids, dipole movement is usually restricted to the point where the dipole orientation polarization becomes less significant than the electronic mode. At optical frequencies, only electronic polarization is occurring and the refractive index can be fine-tuned through structure modification, physical aging, and guest doping of polymers. In general, aromatic polymers possess higher refractive indices than aliphatic ones due to better packing and electronic polarizability. Similarly, the incorporation of highly  $\pi$ -conjugated dyes raises a polymer's refractive index. The high-temperature densification of aromatic polymers leads to an increase in refractive index due to the decrease of free volume. The incorporation of fluorine atoms in the polymers can affect the refractive index in three ways simultaneously. First, the increase in free volume, which often accompanies fluorine substitution, may decrease the refractive index attributed to the greater steric volume of fluorine relative to hydrogen, which may interfere with efficient chain packing. Second, the electronic polarizability is always lowered with fluorine substitution because of the smaller electronic polarization of the C–F bond relative to C–H bond. And last, the larger difference between the measuring optical wavelengths and the blue-shifted absorption wavelength  $\lambda_{\text{max}}$  (due to fluorine substitution) also contributes to the lowering of the refractive index.

As a result, an important feature of polymers is the controllability of the refractive-index contrast, which can have values of up to 35 %, enabling high-density compact waveguiding structures with small radii of curvature. Compact structures are critical for the achievement of large-scale photonic integration.

**Birefringence:** The birefringence ( $n_{\text{TE}} - n_{\text{TM}}$ ) (TE = transverse electric, TM = transverse magnetic) indicates the optical

anisotropy of a material. In an isotropic material, birefringence is also related to the stress build-up within the material due to processing or thermal treatment. Conventional techniques used for measuring the TE and TM indices of a film with a prism coupling apparatus can only detect large birefringence in some materials. A very sensitive technique of evaluating the birefringence consists of measuring the polarization splitting in the reflection spectrum of a Bragg grating made of the material. In the case when the two reflections overlap too much to be readily resolved, the grating can be heated or cooled, which causes the reflections of the two polarizations to shift at different rates, and broadening/narrowing occurs. By evaluating the difference between the minimum reflection peak width and the width at the temperature where the birefringence value is to be measured, an accurate estimate of the birefringence can be determined. Unlike inorganic crystals or glasses, polymers can be molecularly engineered to achieve low birefringence. Some aromatic polymers, such as polyimides, exhibit a very large birefringence (up to 0.24) that is attributed to the strong preference of aromatic moieties to align with their planes oriented along the film surface.<sup>[11]</sup> However, the birefringence can be extremely low ( $10^{-5}$  to  $10^{-6}$ , the limit of measurement) in polymers that undergo little molecular orientation during processing, as is common in three-dimensionally cross-linked polymers.<sup>[9a]</sup>

**Temperature Dependence:** A fundamental difference between polymeric materials and more conventional optical materials, such as glass, is that their refractive index varies more rapidly with temperature (large thermo-optic (T-O) effect:  $dn/dT$ ). The refractive index of polymers decreases in temperature at a rate of  $10^{-4}/^{\circ}\text{C}$ , which is one order of magnitude larger than that of inorganic glasses. This large T-O coefficient as well as poor thermal conductivity makes it possible to realize T-O switches with low power consumption and digital T-O switches based on adiabatic waveguide transitions, as opposed to the interferometric devices that are necessary in silica-on-silicon, for example. Furthermore, the T-O coefficient is negative, while that of inorganic glass is positive. This characteristic is used in the construction of temperature-independent waveguides. In these waveguides, the small, positive T-O effect in inorganic glass waveguides, used as the core, is canceled out by using the negative T-O coefficient of polymers, used as the cladding. In measuring  $dn/dT$ , an elegant and simple approach is to measure the return loss from the interface between the material to be measured and an optical fiber.<sup>[12]</sup> Such samples can be easily prepared by curing the material around a well-cleaved optical fiber, the other end of which is connected to a return loss meter. If the fiber optical properties are well known, then by simply measuring the change in return loss upon heating, for example, the  $dn/dT$  of the material can be determined.

**Humidity Dependence:** The return-loss technique can also be used to look at the effects of humidity on the refractive index. The humidity-induced change of the refractive index would affect single-mode waveguide performance if core and cladding changes were different; they would also affect the re-

turn loss of the device if index matching were used as the method to reduce return loss. Even in the case where the core and cladding change is the same, if the humidity changes the effective index of the waveguide, it can then affect the performance of devices such as Bragg gratings and AWGs. The humidity dependence of the refractive index in the polymers was ascribed to the counterbalance between moisture absorption and swelling due to the existence of hydrophilic groups. The refractive index of d-poly(methylmethacrylate) (d-PMMA, d = deuterio) increases as the humidity increases at room temperature, while it decreases as the humidity increases at temperatures higher than 60 °C. Although the humidity dependence of d-PMMA is as large as  $10^{-5}$  (% RH)<sup>-1</sup>, some hydrophobic polymers, such as silicone resin, fluorinated epoxy resin, and perfluorinated ether polymer, CYTOP, were affected by humidity to a much lesser degree than the acrylic polymer.<sup>[13]</sup>

**Wavelength Dependence:** Many optical systems rely on having no wavelength-dependent optical effects other than those geometrically designed into the system. Therefore, material dispersion ( $dn/d\lambda$ ) is generally to be avoided. While the values for the polymers on the order of  $10^{-6}$  nm<sup>-1</sup> are comparable to those for SiO<sub>2</sub>, they are much lower than those for semiconductors or doped glasses.<sup>[14]</sup>

### 2.1.2. Optical Loss

In general, all optical waveguide devices need to have low optical loss, especially at the major telecom wavelengths (1310 and 1550 nm) and datacom wavelength (840 nm). With the utilization of fiber-optic telecommunications in the S-band (1450–1510 nm), C-band (1525–1560 nm), and L-band (1570–1620 nm), all optical waveguide devices should possess low loss in these bands. There are several sources of optical loss including absorption, scattering, polarization dependence, reflections, radiation, and fiber coupling.<sup>[15]</sup> Optical polymers have promising characteristics to reduce all of these kinds of loss.

**Absorption Loss:** For polymer materials, both electronic and vibrational absorptions are likely to contribute to optical loss. Polymeric media generally have large absorptions in the ultraviolet owing to fundamental excitations of their electrons. These absorptions tend to be in the deep ultraviolet (less than 200 nm) for polymers with predominantly aliphatic hydrogen atoms, and in the near UV (200–400 nm) for polymers with significant numbers of aromatic hydrogens. Partially or fully fluorinated polymers tend to have their UV absorptions at higher energies. For energies well below electronic energy levels of the polymer, where the polymer is basically transparent, weak absorption can result from a number of sources including singlet–triplet absorption, and vibration mediated absorption inharmonic interactions. In general, electronic absorptions in polymers, with the viable exception of highly colored electro-optic polymers, are very unlikely to contribute significantly to optical losses in the major telecommunications windows near 1300 nm and 1550 nm.

In the 1300–1600 nm range, absorptions coming from the overtones of fundamental molecular vibrations are dominant.<sup>[16]</sup> Since the strength of the absorption tends to decrease by approximately an order of magnitude between each harmonic order, higher harmonics are generally weak enough to not be of concern (at least for waveguide applications). Clearly, the highest energy vibrations will be those that have high spring constants (stiff bonds, such as double bonds) and/or small reduced masses. The smallest reduced mass occurs when one of the atoms is hydrogen, and the C–H aliphatic bond is typically used as the benchmark for infrared absorptions; its absorption is located at 3390 nm. Table 2 provides a comparison of the positions and intensities of various vibra-

Table 2. Wavelengths and intensities of some important vibrational overtones.

Bond	Overtone order	Wavelength [nm]	Intensity (relative)
C–H	1	3390	1
C–H	2	1729	$7.2 \times 10^{-2}$
C–H	3	1176	$6.8 \times 10^{-3}$
C–D	3	1541	$1.6 \times 10^{-3}$
C–D	4	1174	$1.3 \times 10^{-4}$
C–F	5	1626	$6.4 \times 10^{-6}$
C–F	6	1361	$1.9 \times 10^{-7}$
C–F	7	1171	$6.4 \times 10^{-9}$
C=O	3	1836	$1.2 \times 10^{-2}$
C=O	4	1382	$4.3 \times 10^{-4}$
C=O	5	1113	$1.8 \times 10^{-5}$
O–H	2	1438	$7.2 \times 10^{-2}$

tional overtone absorptions of interest when considering optical polymers. Both C–H and O–H overtones are seen to be highly absorptive in the telecommunications windows, whereas C–F overtones, for example, show extremely low absorption throughout the range of interest, owing to their higher harmonic order. As hydrogens are removed through partial fluorination, the absorption of optical polymers reduces significantly. A good empirical quantity with which to compare different polymers is the molecular weight per hydrogen for the monomeric unit, which in the case of PMMA is approximately 12. For highly fluorinated optical polymers, this ratio can be well over 100 (and obviously goes to infinity for perfluorinated materials).

In general, it is difficult to directly determine the absorption of an optical material, since, as discussed in detail below, scattering contributions to the overall attenuation are often indistinguishable from those coming from absorption. The one signature that distinguishes absorption from scattering is the inevitable generation of heat in the absorption process. This observation has served as the basis for several unique techniques, the most relevant of which is photothermal deflection spectroscopy (PDS).<sup>[17]</sup> PDS has been applied to the measurement of absorption in a number of important optical polymer systems. Optical polymers can be highly transparent, with absorption loss values below 0.1 dB cm<sup>-1</sup> at all the key communication wavelengths.

**Scattering Loss:** There are numerous extrinsic contributions to scattering loss in optical materials. Chief among these are

large inclusions such as particles, voids, cracks, and bubbles. Generally, an inclusion is considered large if it is greater than 1  $\mu\text{m}$  in diameter, in which case the scattering intensity is largely wavelength independent. Extrinsic scattering in polymers can result from unfiltered particles, dust, dissolved bubbles, and unreacted monomer. For extrinsic scattering to be eliminated it is necessary to follow rigorously clean procedures in the preparation of polymer formulations, and to perform all coating operations in a clean room. Intrinsic scattering results from density fluctuations and compositional inhomogeneities, both of which occur on very short length scales (0.1  $\mu\text{m}$  or less). Polymer waveguides are typically formed by spin-coating processes in which polymers are deposited from solution and subsequently dried by heating in an oven or on a hot plate. The resulting films are generally uniform, but can have a roughness that will contribute to scattering losses. For a slab waveguide, a loss of 0.03  $\text{dB cm}^{-1}$  can be achieved by reducing the rms roughness of the cladding/core interfaces to 0.04  $\mu\text{m}$ . Single-mode channel waveguides are typically made by a photolithographic process in which wet or dry etching defines the waveguide. Therefore, these etch processes must be performed well enough to keep the surface roughness well below 40 nm or so, to obtain waveguides with propagation losses on the order of 0.03  $\text{dB cm}^{-1}$  or less. When thin films are deposited on substrates, an important aspect of the process is managing the stress that can develop. For planar glass waveguides, depositions are performed at high temperatures and there are subsequent annealing operations that also occur at high temperatures (on the order of 1000  $^{\circ}\text{C}$ ). Polymer waveguides are ordinarily deposited at low temperatures, but solvent bakes and annealing often occur at moderately high temperatures (several hundred degrees centigrade). These temperature excursions, when coupled with the coefficient of thermal expansion (CTE) mismatch that exists between the film and the substrate, result in stress-induced scattering. As scattering often comes from a number of sources, experimental scattering data is often fit with an empirical law of the form:

$$\alpha_{\text{scatter}} = A + B/\lambda^2 + D/\lambda^4 \quad (1)$$

where  $A$  is the contribution from large particle scattering (i.e.,  $\gg \lambda$ ),  $B$  the contribution from inhomogeneities on the order of  $\lambda$  in size (Mie scattering), and  $D$  the contribution from small inhomogeneities ( $\ll \lambda$ , Rayleigh-like). This expression can be used to help deduce the source of the scattering loss if the loss can be measured at several well-separated wavelengths.

The scattering loss can be minimized in polymer waveguides by using direct photopatterning as opposed to surface-roughness-inducing reactive ion etching (RIE). It also can be reduced by ensuring the homogeneity of the medium (for example, no abrupt refractive-index variations caused by phase separation or particles) and by minimizing intrinsic stresses. As opposed to planar silica technologies, polymer technologies can be designed to form stress-free layers regardless of the substrate composition, which can be silicon, glass, quartz,

plastic, or glass-filled epoxy printed-circuit board substrate. Moreover, these films can essentially be free of stress-induced scattering loss when operating above the glass-transition temperature ( $T_g$ ) in cross-linked polymer systems.

For channel waveguides, propagation-loss measurements are almost exclusively performed using the cutback technique. However, as discussed above, losses in channel waveguides come from a number of sources, including the patterning process for the channels (both roughness and stress-induced losses by the patterning process). Therefore, it is useful to have some measure of the slab waveguide loss, as this will isolate the sources of loss to absorption, extrinsic scattering, film roughness, and stress-induced scattering resulting from the film deposition process. There are two primary methods, the scanning fiber technique and the liquid prism. The major advantages of the scanning fiber technique are that it can be performed easily on any slab waveguide sample and it does not require extensive handling of the sample (just the coupling to the input prism). The biggest drawback to this method is that if the sample is not clean or has a minute amount of large particles, these defects will scatter significant amounts of light, causing the baseline for the analysis to vary greatly. However, for clean samples without defects this method can achieve accuracies of less than 0.5  $\text{dB cm}^{-1}$ . A common alternative approach to slab waveguide loss measurements is the moving prism technique, where a fixed in-coupling prism is used in conjunction with a movable out-coupling prism to achieve a measurement of transmission vs. propagation length. However, this method and its variations usually suffer from uncertainty with regard to the coupling loss as the out-coupling prism is moved from position to position. This uncertainty limits the accuracy of the technique. A novel approach to improving the accuracy is to adopt a liquid out-coupling prism.<sup>[18]</sup> With this technique, accuracies well below 0.1  $\text{dB cm}^{-1}$  are routinely achieved.

**Polarization-Dependent Loss:** Polarization-dependent loss (PDL) is the maximum difference of attenuation between any of the two polarization states. Frequently, for straight planar waveguides, PDL is the difference between the TE and TM loss. However, for devices, PDL is commonly defined as the maximum difference of loss between the elliptical polarization states, and it can also vary among the various types of optical devices. The TE loss measured in planar waveguides can be higher than the TM loss when the vertical walls of the core have a higher degree of roughness than the horizontal boundaries, and it can be lower when the vertical evanescent tails overlap with an absorptive substrate or "superstrate". An additional source of PDL is the stress mentioned above, which can directly or indirectly lead to increased losses along either the TE or TM direction depending on the nature of the stress. By having a minimal edge roughness, a well-confined material stack, and low-stress processing a well-optimized waveguide can have PDL values that are very small, provided that the waveguide material itself has a low birefringence.

**Insertion Loss:** Insertion loss is defined as  $-10 \log_{10}(P_{\text{out}}/P_{\text{in}})$  with  $P_{\text{in}}$  the input and  $P_{\text{out}}$  the output power from partic-

ular ports of an optical device. Acceptable insertion loss is determined by the overall system loss budget, which will be a function of transmitter power, optical amplifier gain, and receiver sensitivity among other factors. The total insertion loss achieved in planar polymer components can approach the value of the material absorption loss when fabrication techniques are optimized.

**Return Loss:** Return loss is defined as  $-10 \log_{10}(P_{\text{refl}}/P_{\text{in}})$  with  $P_{\text{refl}}$  the reflected and  $P_{\text{in}}$  the input power to the device. Return loss should be minimized both to improve the insertion loss and to prevent reflected light from traveling back up the transmission system or network, where it can have destabilizing and damaging effects on lasers, especially when passing through bi-directional amplifiers.

**Radiation Loss and Fiber Pigtail Loss:** The radiation loss can be reduced by using standard integrated-optic design rules such as large radii of curvature and adiabatic modal transitions. The fiber pigtail loss can be minimized by matching the mode of the planar waveguide to that of the fiber, which can be achieved by tuning the index contrast, the index profile, and the core dimensions. It can also be minimized by optimizing the alignment of the waveguides to the fiber, and by minimizing the Fresnel reflections with appropriate index-matching materials at the interfaces.

### 2.1.3. Processibility and Mechanical Properties

Optical polymers provide for the flexible, large-area, and low-cost fabrication of waveguide devices through simple spin-coating techniques, low-temperature processing, and compatibility with semiconductor electronics. A wide range of rigid or flexible substrates can be used, including glass, quartz, oxidized silicon, glass-filled epoxy printed circuit board substrate, and flexible polyimide film. By controlling the polymer/solvent ratio and the spin speed of film coating, film thicknesses can be obtained in the range of 0.1 to 100  $\mu\text{m}$ . Unlike other optical material systems, polymers are designed and synthesized by chemical modification of constituent molecules to have the desired characteristics, such as melt or solution processibility in the form of monomers or prepolymers, photo- or thermo-crosslinking-enhanced mechanical properties, and matched refractive index between core and cladding layers. Furthermore, these properties are adjustable through formulation variations. There are several polymer waveguide formation techniques such as direct lithographic patterning, soft lithography, embossing, molding, and casting in addition to the conventional photoresist patterning. This permits the rapid, low-cost shaping for both waveguide formation and material removal for grafting of elements such as active films, Faraday rotators, or half-wave plates. This flexibility also makes polymers an ideal hybrid integration platform, where foreign material systems, such as YIG (yttrium iron garnet) and lithium niobate, and semiconductor devices, such as lasers, detectors, and logic circuits, can be inserted into an etched groove in a planar light-wave circuit to enable full amplifier modules or optical add/drop multiplexers on a single

substrate. Moreover, the combination of flexibility and toughness in optical polymers makes them suitable for vertical integration to realize 3D and even all-polymer integrated optics.

### 2.1.4. Environmental Performance

**Thermal Stability:** An important characteristic for practical applications is the thermal stability of optical properties because polymeric materials are subject to yellowing upon thermal aging. Typically, such aging results from the formation of partially conjugated molecular groups characterized by broad ultraviolet absorption bands, which tail off in intensity through the visible region. This yellowing is strongly influenced by the chemical structure of the original polymer. The chemical structures of various backbone segments in the optical polymers can vary substantially from simple aliphatic to aromatic, and linkages can vary from ether, to ester or urethane. The choice of these linkages and monomers or oligomers ultimately determines to a significant degree the characteristics of the resulting polymer, including surface energy, hardness, toughness, modulus, water uptake, and stability toward aging. In fully halogenated materials, yellowing becomes almost negligible at any wavelength because the absence of hydrogen prohibits the formation of H-halogen products that will result in carbon double bonds. These unsaturated double bonds are the major cause of yellowing when they are slowly oxidized under long-term thermal aging.

**Telecordia GR1209 and GR1221:** Requirements for telecommunications network devices have been developed with the goal of assuring operation for 20 to 25 years. The major governing documents for passive optical components are two monographs from Telecordia, the GR1209 and GR1221. The Telecordia GR1209 focuses primarily on optical performance tests and short-term reliability data (several weeks) that would apply to any manufactured lot of devices<sup>[19]</sup> (Table 3). The Telecordia GR1221 is a document that focuses on comprehensive reliability assurance, in particular vendor and device qualification, lot-to-lot quality and reliability control, storage, and handling<sup>[20]</sup> (Table 4). Of particular concern for polymers are extreme temperatures and humidities, as well as the broad range of temperatures that may bracket either the  $T_g$  or the sub- $T_g$  relaxations of the polymer. However, polymers that stand up to 85 °C and 85 % RH (relative humidity)

Table 3. Telecordia GR1209 required environmental and mechanical tests.

Test	Condition
Temperature humidity aging	85 °C/85% RH for 14 days
Temperature humidity cycling	−40 °C to 75 °C, 10% to 80% RH, 42 cycles, 14 days
Water immersion	43 °C, pH 5.5, 7 days
Vibration	10–55 Hz, 1.52 mm, 2 h
Flex test	1 lb load, 100 cycles
Twist test	1 lb load, 10 cycles
Side pull	0.5–1 lb load, 90° angle, active
Cable retention	1.2–2.2 lb load for 1 month
Impact test	6 ft. drop, 8 cycles, 3 axes

Table 4. Telecordia GR1221 required environmental tests.

Test	Condition
High temperature storage (damp heat)	75 °C/90% RH for 2500 h
High temperature storage (dry heat)	85 °C, <40% RH for 2500 h
Low temperature storage	−40 °C, uncontrolled RH for 2500 h
Temperature cycling	−40 to 75 °C, dwell ≥ 15 min, ramp @ 1 °C/min, 500 cycles
Temperature/humidity cycling	25 °C/uncontrolled RH to 75 °C/90%, 4 to 16 hrs dwell, ramp @ 2 °C/min, 5 cycles
Thermal shock	$T = 100$ °C, dwell ≥ 30 min, transfer 2 min, 20 cycles
Salt spray	$T = 35$ °C, 5% NaCl dissolved in 95% H <sub>2</sub> O, 168 h
Water immersion	43 °C, pH 5.5, 340 h

conditions have been demonstrated, and some polymers have already passed the Telecordia GR1209 and GR1221 environmental tests. Extensive materials research has yielded polymers that are highly reliable, to the extent that they are no longer the limiting factor in component lifetime.

## 2.2. Conventional Optical Polymers

The preparation of light-guiding films with polymers started in the 1970s.<sup>[21]</sup> Table 5 summarizes the characteristics of conventional optical polymers such as poly(methylmethacrylate) (PMMA),<sup>[22]</sup> polystyrene (PS),<sup>[23]</sup> polycarbonate (PC),<sup>[24]</sup> polyurethane (PU),<sup>[25]</sup> and epoxy resin.<sup>[26]</sup>

Table 5. Properties of conventional optical polymers.

Material	Refractive index ( $n$ )	$T_g$ [°C]	Loss [dB/cm]
PMMA	1.49	105	0.2 (at 850 nm)
PS	1.59	100	
PC	1.58	145	
PU	1.56		0.8 (at 633 and 1064 nm)
Epoxy resin	1.58		0.3 (at 633 nm), 0.8 (at 1064 nm)

These polymers possess very different structures, for example, PMMA with an aliphatic backbone and ester side-chain, PC with an ester backbone, and polyurethane with an amino-ester backbone. As a result, their properties vary significantly in the aspects of refractive index, optical loss, and thermal stability.<sup>[27]</sup>

## 2.3. Novel Optical Polymers

In the past twenty years, several major families of novel optical polymers have been developed in academic and industrial laboratories. Some are even available commercially<sup>[28]</sup> (Table 6). These polymers can be grouped into four major classes: deuterated and halogenated polyacrylates,<sup>[29]</sup> fluorinated polyimides,<sup>[30]</sup> perfluorocyclobutyl (PFCB) aryl ether

polymers,<sup>[31]</sup> and nonlinear optical polymers.<sup>[32]</sup> Other important but less explored optical polymers include benzocyclobutene (BCB),<sup>[33]</sup> perfluorovinyl ether cyclopolymer (CYTOP),<sup>[34]</sup> tetrafluoroethylene and perfluorovinyl ether copolymer (Teflon AF),<sup>[35]</sup> silicone,<sup>[36]</sup> fluorinated poly(arylene ether sulfide),<sup>[37]</sup> poly(pentafluorostyrene),<sup>[38]</sup> fluorinated dendrimers,<sup>[31e]</sup> and fluorinated hyperbranched polymers.<sup>[39]</sup> Currently, the available optical polymers are highly transparent with absorption loss values below  $0.1 \text{ dB cm}^{-1}$  at all major communication wavelengths (840, 1310, and 1550 nm).

### 2.3.1. Deuterated and Halogenated Polyacrylates

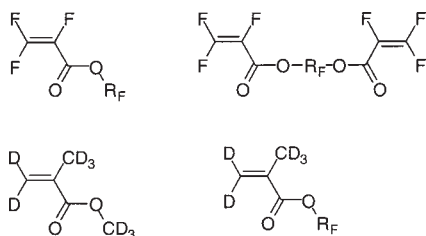
Primarily, deuterated or halogenated polyacrylates were developed by Allied-Signal (recently merged with Honeywell), NTT, and Dupont. Allied-Signal developed a wide variety of photo-crosslinkable, optically transparent polymers based on the combinations of multifunctional halogenated acrylate monomers and oligomers in addition to various additives.<sup>[29]</sup> These polymers are particularly suitable for practical low-loss optical devices because acrylates have intrinsically very low stress-optic coefficients. Moreover, since these polymers can be photochemically processed directly from their neat monomers, it provides the resulting polymers with fairly low internal stress and dimension shrinkage. This combination of material properties allows the creation of waveguides with low scattering losses and low polarization-dependent losses. Upon exposure to actinic radiation (e.g., UV or e-beam), these monomer systems form highly crosslinked networks, which exhibit low intrinsic absorption in the wavelength range extending from 400 to 1600 nm. By blending and copolymerizing with selected miscible monomers, this approach allows precise tailoring of the refractive index over a very broad range from 1.3 to 1.6, although it can be difficult to simultaneously achieve a given refractive index and low intrinsic absorption at the same time. This control of refractive index allows researchers to fabricate step-index or graded-index optical waveguide structures with well-defined and reproducible refractive index differences ( $\Delta n$ ) to within 0.0001. At the same time, this synthetic approach allows other physical properties of the materials such as flexibility, toughness, surface energy, and adhesion to be tailored to meet the needs of specific applications. These materials have already passed most of the Telecordia protocols GR1209 and 1221. NTT has developed deuterated polyfluoromethacrylate (Scheme 1) with high transparency, low birefringence, and good processability. They have also developed processes to fabricate low optical loss single-mode and multi-mode optical waveguides with these polymers. The propagation loss and waveguide birefringence of the single-mode waveguides were as low as  $0.10 \text{ dB cm}^{-1}$  and  $-5.5 \times 10^{-6}$  at  $1.31 \mu\text{m}$ , respectively. The propagation losses of the multi-mode waveguides were less than  $0.02 \text{ dB cm}^{-1}$  at both 0.68 and  $0.83 \mu\text{m}$ , and  $0.07 \text{ dB cm}^{-1}$  at  $1.31 \mu\text{m}$ . Polyguide, developed by DuPont and licensed to AMP, has shown excellent layer quality and thickness control. Buried waveguide circuitry can be formed with relatively low

Table 6. Characteristics of novel optical polymers developed globally by companies.

Company	Polymer type	Patterning techniques	Propagation loss, single-mode waveguide [dB/cm] (wavelength, [nm])	Other properties (wavelength, [nm])
Optical Crosslinks (formerly DuPont and Polymer Photonics)	Acrylate (Polyguide)	Diffusion	0.18 (800) 0.2 (1300) 0.6 (1550)	Laminated sheets Excimer-laser machinable
Corning (formerly AlliedSignal)	Acrylate	Photoexposure/ wet etch, RIE, laser ablation	0.02 (840) 0.3 (1300) 0.8 (1550)	Birefringence: 0.0002 (1550) Crosslinked, $T_g$ : 25 °C Environmentally stable
	Halogenated acrylate	Photoexposure/ wet etch, RIE, laser ablation	0.01 (840) 0.06 (1300) 0.2 (1550)	Birefringence: 0.000001 (1550) Crosslinked, $T_g$ : -50 °C Environmentally stable
NTT	Halogenated acrylate	RIE	0.02 (830) 0.07 (1310) 1.7 (1550)	Birefringence: 0.000006 (1310) $T_g$ : 110 °C
	Deuterated polysiloxane	RIE	0.17 (1310) 0.43 (1550)	Environmentally stable
	Fluorinated polyimide	RIE	TE:0.3, TM: 0.7 (1310)	PDL: 0.4 dB/cm (1310) Environmentally stable
Amoco	Fluorinated polyimide (Ultradel)	Photoexposure/ wet etch	0.4(1300) 1.0 (1550)	Birefringence: 0.025, crosslinked, thermally stable
General Electric	Polyetherimide (Ultem)	RIE, laser ablation	0.24 (830)	Thermally stable
Hitachi	Fluorinated polyimide	Photoexposure/ wet etch	TE: 0.5, TM: 0.6 (1300)	Birefringence: 0.009 (1300), PDL: 0.1 dB/cm (1300), $T_g$ : 310 °C, thermally stable
Dow Chemical	Perfluorocyclobutane (XU 35121)	Photoexposure/ wet etch	0.25 (1300) 0.25 (1550)	$T_g$ : 400 °C
	Benzocyclobutene (Cyclotene)	RIE	0.8 (1300) 1.5 (1550)	$T_g$ : > 350 °C
Asahi Glass	Perfluorovinyl ether cyclopolymer (CYTOP)			$n = 1.34$ $T_g$ : 108 °C
DuPont	Tetrafluoroethylene and perfluorovinyl ether copolymer (Teflon AF)			$n = 1.31$ (AF 1600) $n = 1.29$ (AF 2400)
JDS Uniphase (formerly Akzo Nobel) Telephotonics	Polycarbonate (BeamBox) (OASIC)	RIE	0.6 (1550)	Thermally stable
		Photoexposure/ wet etch, RIE, laser ablation	< 0.01 (840) 0.03 (1300) 0.1 (1550)	Environmentally stable
Gemfire	(Gemfire)	Photoexposure/ wet etch	1.0 (1550)	Birefringence: 0.0002 (1550) Crosslinked
K-JIST	Fluorinated poly(arylene ether sulfide) (FPAESI)	RIE	TE: 0.42, TM: 0.4 (1550)	Birefringence: 0.0003 (1550), PDL: 0.02 dB/cm (1550), crosslinked, thermally stable
Redfern	Inorganic polymer glass (IPG)	RIE		Environmentally stable
Hoechst Celanese	PMMA copolymer (P2ANS)	Photobleaching	1.0 (1300)	NLO polymer
PacificWave	Polycarbonate with CLD-1 chromophore (PC-CLD-1)	RIE	1.8 (1550)	NLO polymer, $r_{33} = 70$ pm/V (1310), pigtail loss=1.5 dB/facet
Lumera	Polyurethane with FTC chromophore (PU-FTC)	RIE	2.0 (1330)	NLO polymer, $r_{33} = 25$ pm/V (1310), pigtail loss = 5 dB/facet
Ipitek	Poly(methylmethacrylate) with CLD-1 chromophore (PMMA-CLD-1)	RIE	5.0 (1300)	NLO polymer, $r_{33} = 60$ pm/V (1300), pigtail loss=3.5 dB/facet

optical losses using photolithographic patterning and lamination techniques. In addition, Polyguide can be machined using excimer lasers to form mechanical structures with a high de-

gree of accuracy allowing for connection to an mechanically transferable (MT-type) ferrule packaged with push/pull housing connected to a multichannel standard ribbon fiber. Poly-

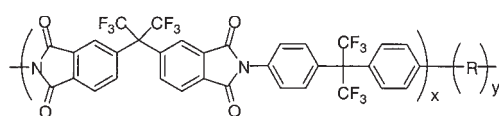


Scheme 1. Structures of deuterated and fluorinated acrylate monomers.

guide possesses high refractive indices (1.48 to 1.51) and high optical losses ( $0.18 \text{ dB cm}^{-1}$  at  $0.8 \mu\text{m}$ ,  $0.2 \text{ dB cm}^{-1}$  at  $1.3 \mu\text{m}$ , and  $0.6 \text{ dB cm}^{-1}$  at  $1.55 \mu\text{m}$ ) due to its non-halogenated acrylate structures.

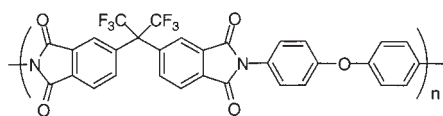
### 2.3.2. Fluorinated Polyimides

Although acrylate-derived polymers have demonstrated many attractive properties as discussed above, they do not possess the needed thermal stability (as high as  $300^\circ\text{C}$ ) for direct on-chip interconnect applications. In this regard, polyimides are a proven class of polymers in the microelectronics industry due to their high thermal stability ( $>300^\circ\text{C}$ ) and outstanding dielectric and mechanical properties.<sup>[40]</sup> However, conventional polyimides used in the semiconductor industry have poor characteristics that make them unsuitable for use as optical materials. In the past decade, several types of fluorinated polyimides (Scheme 2) that feature low optical losses in

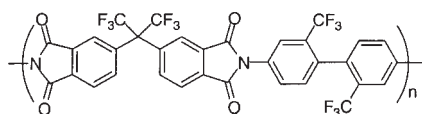


R: alkylated photocrosslinking group

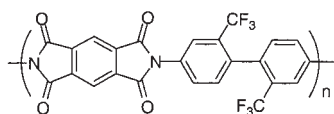
Ultradel 9020D



Amoco 4212



6FDA/TFDB



PMDA/TFDB

Scheme 2. Some representatives of fluorinated polyimides.

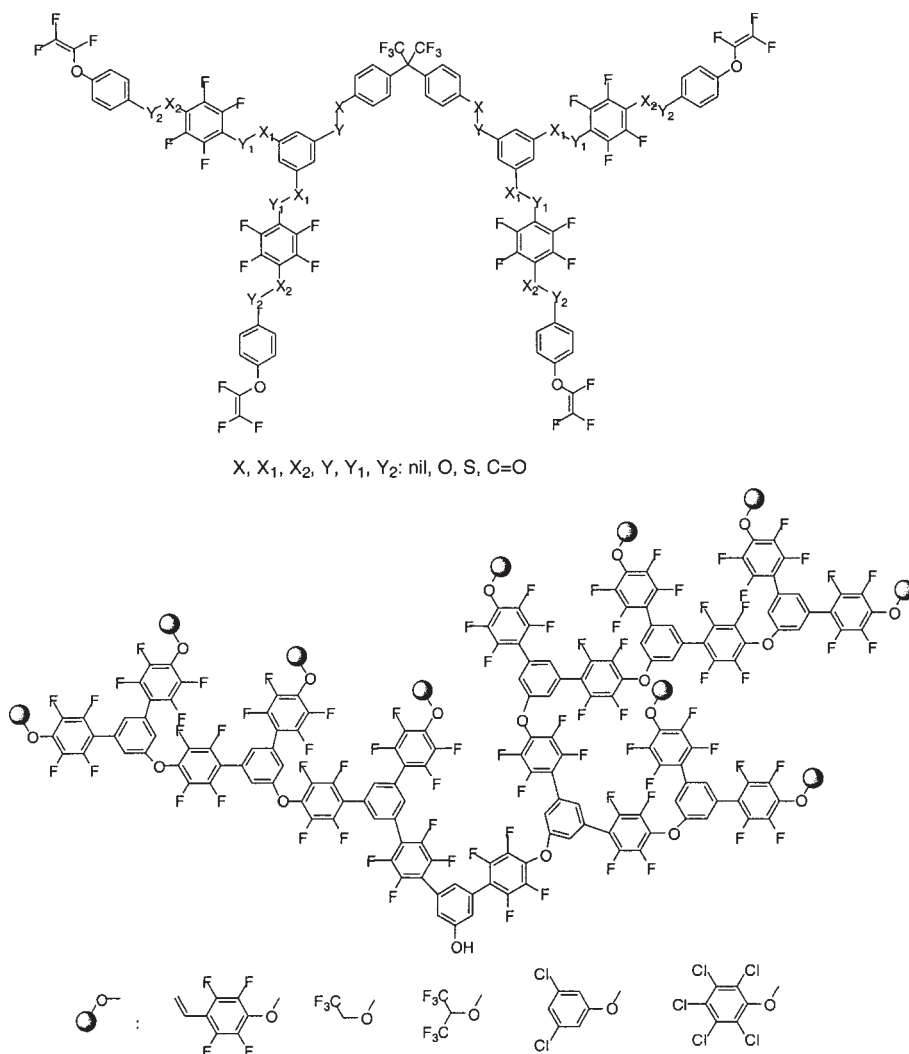
the near infrared region, a broad range of refractive index control, and excellent heat resistance have been introduced by Amoco (Ultradel), General Electric (Uitem), NTT, and Hitachi.

For polyimides, there are two main causes for the observed waveguide losses.<sup>[41]</sup> Firstly, ordering processes can lead to refractive index fluctuations producing scattering centers (domain formation/phase separation). Furthermore, ordering can favor the formation of charge-transfer complexes, thus leading to increased absorption. Secondly, the evaporation of complexed (through H-bonding) or trapped casting solvents as well as water produced during imidization can cause voids or pinholes in the optical waveguide. Optical loss produced by the latter mechanism can be reduced by optimizing the curing procedure. However, it is also observed that annealing allows ordering to occur and thus introduces charge complexation and refractive-index fluctuations to exhibit high loss values, and rapid heating leads to increased optical losses accompanied by a small change in the absorption spectrum. As a result, it is assumed that the losses introduced by rapid curing are due to voids and/or pinholes whereas the losses introduced by annealing above the glass-transition temperature of the polyimide might originate from residual chain-chain interactions. Nevertheless, most of the ordering processes so typical for conventional polyimides seem to be suppressed in fluorinated polyimides.<sup>[30]</sup> Therefore, these materials allow the production of thermally stable waveguides with low optical losses. One intrinsic problem that is still difficult to avoid, however, is the large birefringence and polarization dependent loss (PDL) that results from aromatic ordering in the polyimides.

### 2.3.3. Perfluorocyclobutyl Aryl Ether Polymers

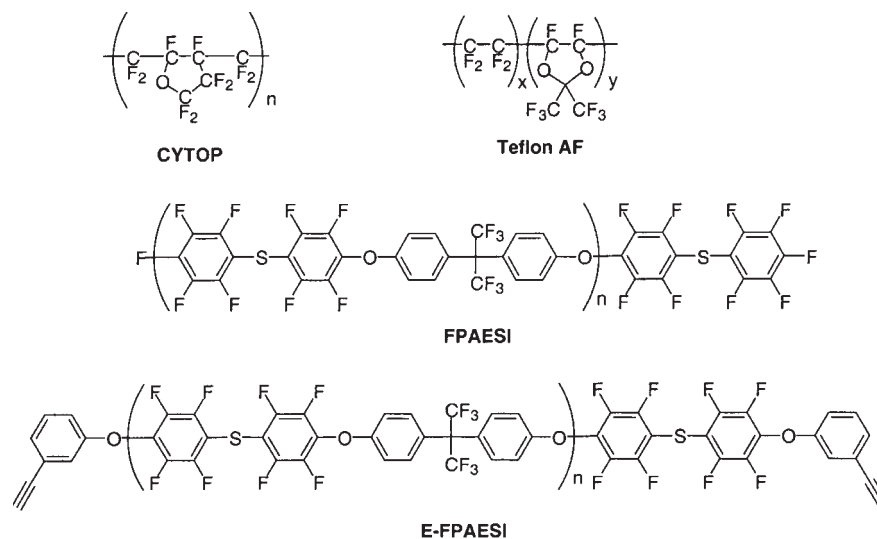
For most spin-coating applications, the solubility of optical polymers or oligomers needs to exceed 50 wt.-% in common solvents if a reasonable film thickness and planarity is to be obtained. Such basic requirements severely limit the use of many fluoropolymers based on chain addition polymerization as well as polyimide condensation polymers. However, poly(aryl ether) polymers based on perfluorocyclobutyl (PFCB) repeating units, first developed by Dow Chemical, possess both high-performance properties and processibility.<sup>[31]</sup> These polymers are synthesized through the thermal cyclopolymerization of trifunctional and bifunctional aryl trifluorovinyl ether monomers to PFCB copolymers. PFCB polymers and copolymers possess a unique combination of properties well suited for optical applications such as high temperature stability, precisely controlled refractive index, low moisture absorption, excellent melt and solution processibility, a high thermo-optic coefficient, and low absorption at 1300 and 1550 nm. Copolymerization reactions also offer tailored thermal and optical properties in these polymers by simply choosing suitable co-monomers. PFCB polymers can be solution or melt microfabricated via standard methods or be processed by soft-lithographic techniques. Recently, thermal properties





Scheme 4. Crosslinkable fluorinated dendrimers and hyperbranched polymers.

tical fibers at both visible and infrared wavelengths (Scheme 5). However, due to their high hydrophobicity and low refractive index, there are some limitations for using these polymers for optical waveguide applications, such as: 1) difficulty in integrating them in multilayer waveguide structures due to poor adhesion, 2) maintenance of overall dimensional or thermo-mechanical stability, and 3) difficulty in waveguide processing using established fabrication techniques. Although these problems are typically viewed as secondary issues after the primary performance, the latter limitation of processibility can be most critical when real production is considered.



Scheme 5. Other typical fluorinated polymers.

### 2.3.6. Electro-optic Polymers

Electro-optic (E-O) polymers have been intensively investigated and developed during the past two decades. However, due to the difficulty of obtaining thermally stable and mechanically robust E-O polymers to fulfill the stringent requirements needed for processing and operating of E-O devices, the development of E-O polymers has become quite stagnant. Recently, due to the rapid development of photonic technologies and the ever-increasing demand of faster switching speed and higher bandwidth in telecommunications, several companies, including PacificWave, Lumera, and Lockheed Martin, have exerted significant effort in trying to commercialize optical waveguide devices such as E-O modulators and switches based on E-O polymers.

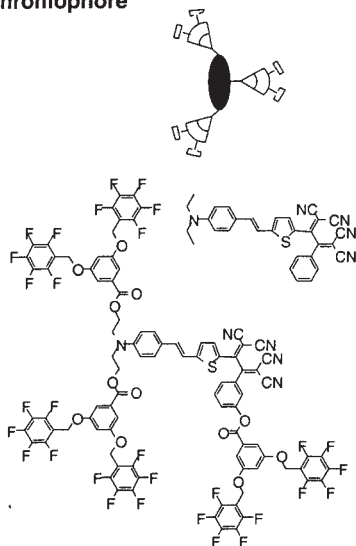
It is well known that the second-order nonlinear optic (NLO) properties originate from non-centrosymmetric alignment of NLO chromophores, either doped as a guest or covalently bonded as side-chains in poled polymers.<sup>[32a,32g-i]</sup> To obtain device-quality materials, three stringent issues must be addressed: 1) design and synthesis of high  $\mu\beta$  ( $\mu$ : the chromophore dipole moment,  $\beta$ : the

molecular first hyperpolarizability) chromophores and realization of large macroscopic E-O activity in the chromophore-incorporated polymers; 2) maintenance of long-term temporal stability in the E-O response of the poled materials in addition to their high intrinsic stability toward the environment such as heat, light, oxygen, moisture, and chemicals; 3) minimization of optical loss from design and processing of materials to fabrication and integration of devices.

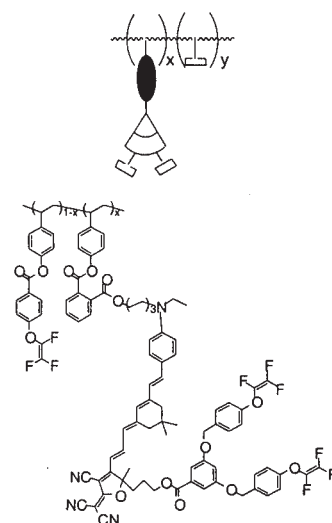
In the context of addressing the first issue, the major task encountered is to efficiently translate the high molecular hyperpolarizability ( $\beta$ ) values of organic chromophores into large macroscopic E-O activity ( $r_{33}$ ) in polymers and also maintain their high thermal stability and low optical loss. Electric field poling of a polymer containing highly nonlinear chromophores is often hindered by the shape-dependent chromophore–chromophore electrostatic interactions through the large dipole moment of the molecules.<sup>[32d]</sup> Recently, several very promising E-O dendritic material systems have been developed, ranging from the 3D shape dendritic chromophore, to the multiple-armed chromophore-containing dendrimers with NLO chromophores connected to the center core with crosslinkable trifluorovinylether as the crosslinkable periphery, to the side-chain dendrimerized NLO polymers<sup>[32e–f]</sup> (Scheme 6). The preliminary results obtained from these dendritic material systems have shown great promise in achieving much higher E-O activities ( $>100 \text{ pm V}^{-1}$ , which is a factor of three larger than the commercial inorganic system, lithium niobate). This approach may provide the new paradigm for the design of highly efficient E-O materials for ultra-low drive-voltage E-O modulators.<sup>[32c]</sup>

In addressing the second issue, two approaches have been adopted to improve the long-term stability of molecular orientation in poled polymers. First, very high- $T_g$  polymers such as polyimide<sup>[32l,m]</sup> and polyquinoline<sup>[32n]</sup> have been used as host matrices to incorporate NLO chromophores. After poling, these guest/host polymers have shown quite promising long-term stability at elevated temperatures. Moreover, the motion of chromophores in polymer matrices can be further restricted when the chromophores are covalently attached to polyimides or polyquinolines either in the form of a main chain or as a side-chain. This approach has led to polymers

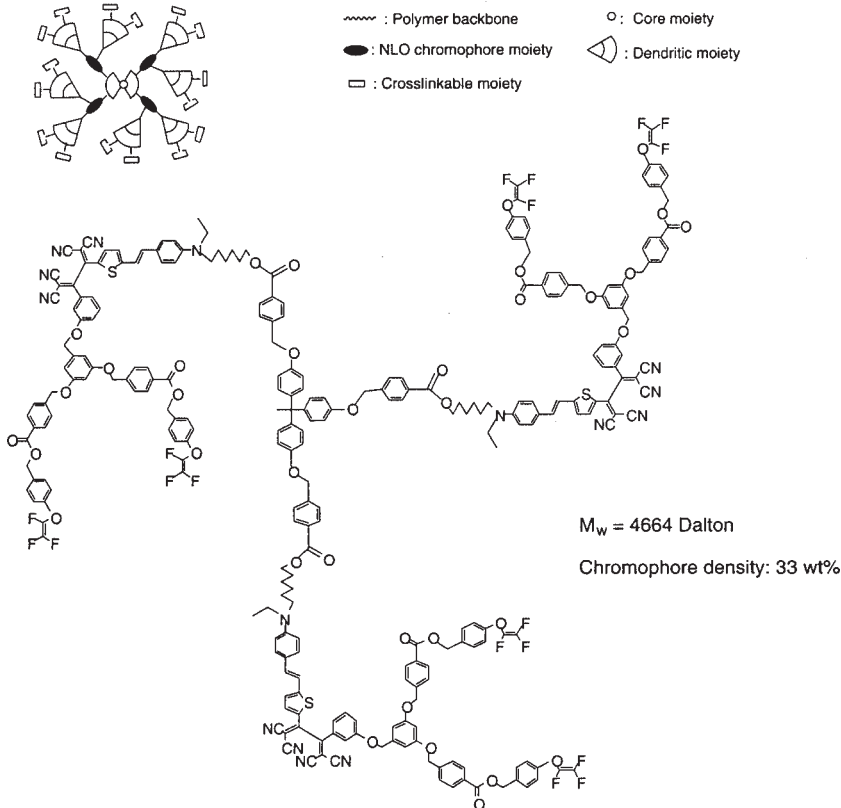
#### Multiple dendron-modified NLO chromophore



#### Crosslinkable dendritic NLO polymer:



#### Crosslinkable multi-chromophore containing NLO dendrimer:



Scheme 6. Dendritic E-O materials.

with exceptional thermal stability.<sup>[32b]</sup> Another alternative approach is to develop a lower- $T_g$  material, which contains reactive functional groups on the chromophore or on the polymer backbone, that can be processed into optical-quality thin films, and can then be poled and crosslinked simultaneously at higher temperatures to lock the chromophores and poly-

mers in place to achieve better control over the poling-induced polar order. The crosslinkable epoxy resins, polyurethanes, polyimides, and poly(perfluorocyclobutyl ether)s (PFCBs) have been used to enhance orientational stability of the poled polymers.

The third critical issue influencing the utilization of polymeric electro-optic materials is that of optical loss at the communication wavelengths of 1.3 and 1.55  $\mu\text{m}$ . Both absorption and scattering of light from materials will contribute to optical loss. However, the scattering loss in E-O polymers can be reduced by controlling the homogeneity of chromophore dispersion in the E-O polymer films before and after poling to avoid phase separation, and the uniformity of the guiding and cladding films in the NLO polymeric waveguide. Minimization of optical loss associated with C–H vibrational absorptions has been the focus of scientists endeavoring to develop low loss passive polymer optical waveguides. Active polymers are unlikely to yield optical losses as low as passive polymers due to the requirement of chromophore incorporation and lattice hardening to lock poling-induced chromophore alignment in acentric order. Partial fluorination of NLO chromophores and the incorporation of chromophores into fluorinated polymers such as PFCB polymers have proved to be a useful approach to minimize the absorption loss of the resulting materials, since the thermosetting reaction involved in PFCB formation does not generate any O–H, N–H, or aliphatic C–H bonds.

### 3. Processing

The techniques and relevant issues for processing polymer optical waveguides are quite similar to those for polymers in microelectronic packaging.<sup>[43]</sup> Common techniques for casting polymer films include spin coating, doctor blading, extrusion, and lamination. The major concerns when fabricating a film are that the film is of uniform thickness, is free of bubbles and striations, will adhere well to the substrate of interest, and that the film can be made to the desirable thickness. Each casting technique has its own advantages and disadvantages. For example, spin coating allows suitable control of thickness and uniformity; however, eliminating striations in films can be difficult. The techniques that have been used for patterning optical waveguides in polymer films include photoresist-based patterning, direct lithographic patterning, and soft lithography. Figure 2 compares photoresist-based patterning and direct lithographic patterning to generate polymer optical waveguides. Micromolding in capillaries (MIMIC) and micro-

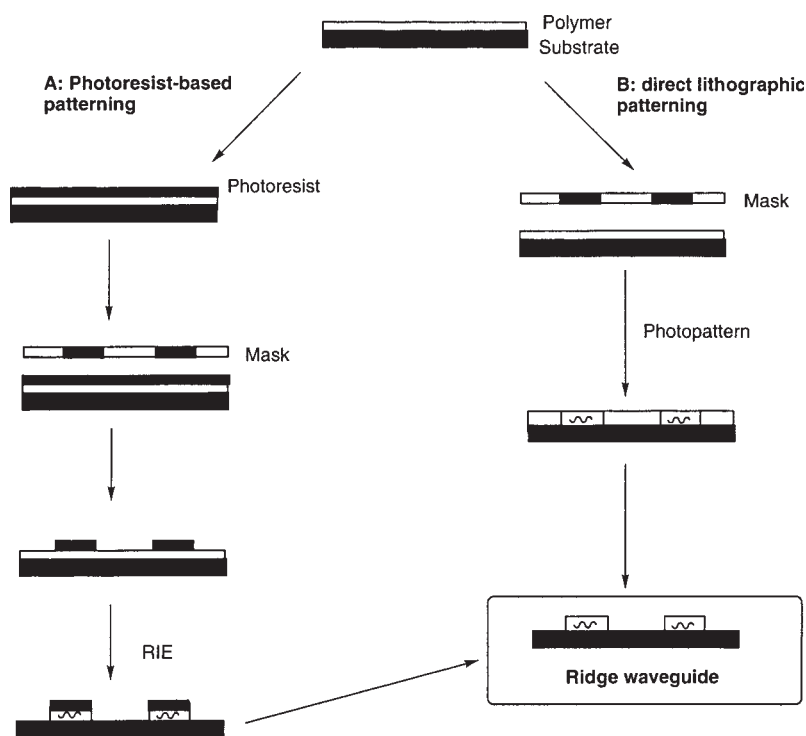


Fig. 2. Comparison of photoresist-based patterning and direct-lithographic patterning to generate polymer optical waveguides.

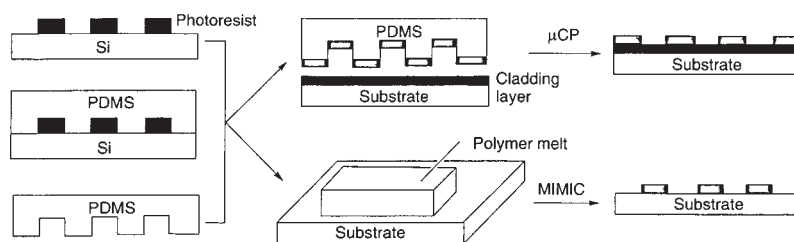


Fig. 3. Micromolding in capillaries (MIMIC) and microcontact print ( $\mu\text{CP}$ ) to generate polymer optical waveguides.

contact printing ( $\mu\text{CP}$ ) to achieve polymer optical waveguides are shown in Figure 3.

#### 3.1. Photoresist-Based Patterning

In general, for the fabrication of polymer optical waveguides standard semiconductor processing technology is adopted, for example, spin-coating, baking, and RIE processes. However, very significant efforts have been made to optimize the waveguide fabrication process, particularly in the areas of deep, smooth, and vertical sidewall etching to minimize optical losses contributed from sidewall scattering. In conventional RIE, only one radiofrequency (rf) power source is applied to regulate both plasma density and ion energy (or direct current bias) and it is impossible to control them separately. Although the etch rate increases with rf power, the in-

creased rf power can cause severe sputtering by energetic ions at the sample surface, leading to increased damage on the sample and decreased etch selectivity. In this regard, high-density plasma etching using an inductively coupled plasma (ICP) source offers an attractive alternative over the conventional RIE. ICP etching uses a secondary rf power source (ICP power) to generate a high-density plasma (typically two to three orders of magnitude higher than that generated by RIE) without correlating to the ion energy. Thus, ICP etching produces low surface damage while achieving high etch rates.<sup>[44]</sup>

### 3.2. Direct Lithographic Patterning

Laser direct-writing can be used to fabricate optical waveguides from photosensitive polymers. The technique of laser direct-writing has the advantage of being maskless, allowing rapid and inexpensive prototyping in contrast to conventional mask-based photolithographic approaches in which a mask must first be designed and fabricated before waveguides can be produced. This technique is capable of patterning features with long and linear dimensions over comparatively large planar areas. This capability is matched to the requirements of producing an array of waveguides and switches, typical of optical switching fabrics, arranged over areas that are large, e.g.,  $\approx 10\text{--}1000\text{ cm}^2$ , in comparison to those characteristic of integrated circuit (IC) dice. However, it can be difficult to form important structures such as splitter Y-junctions and directional couplers with laser direct-writing. Laser-writing can play a role in the fabrication of large dimension parts where masks cannot be produced; for instance, several-meter-long polymer waveguides can easily be laser-written on large substrates such as rolls of flexible plastics.<sup>[45]</sup>

Photobleaching is another kind of direct lithographic patterning and is useful for dye-containing optical polymer systems such as E-O polymers.<sup>[46]</sup> A novel fabrication technique is electron-beam direct-writing,<sup>[47]</sup> which has advantages over the conventional UV-photobleaching technique: 1) since the irradiation is operated in vacuum, the effect of dust can be neglected; 2) this technique can demonstrate the fabrication of a sub-micrometer or even a nanometer pattern with high resolution; 3) a computer-assisted-design system supports the writing of complex patterns for advanced optical devices such as E-O modulators.

### 3.3. Soft Lithography

Microfabrication using non-photolithographic techniques (soft lithography) has been pioneered by Whitesides et al.<sup>[48]</sup> and recently used to fabricate optical waveguides.<sup>[49]</sup> These techniques involve preparation of poly(dimethylsiloxane) (PDMS) molds/stamps by casting PDMS on a photolithographically generated silicon master with the desired micropattern. The PDMS mold, thus obtained, can be used in a variety

of ways to replicate the micropatterns of the polymer on a given substrate. Two such examples, namely microcontact printing and micromolding in capillaries, are shown schematically in Figure 3. Both of the techniques were found to work very well with PFCB polymers.

## 4. Devices

### 4.1. Optical Interconnects for Computing Systems

The speed and complexity of integrated circuits are increasing rapidly from very-large scale integrated (VLSI) circuits to ultra-large scale integrated (ULSI) circuits. As the number of components per chip, the number of chips per board, the modulation speed, and the degree of integration continue to increase, electrical interconnects are facing fundamental bottle-necks, such as speed, packaging, fan-out, and power dissipation. Multichip module (MCM) technology is employed to provide higher clock speeds and circuit densities. However, the state-of-the-art technologies based on electrical interconnects fail to provide the required multi-Gbit/s clock speed and communication distance in intra-MCM and inter-MCM hierarchies. As a result, optical interconnects for MCMs, chips, boards, and backplanes have been recently fabricated.<sup>[50]</sup> Figure 4 shows several typical schematics of optical intercon-

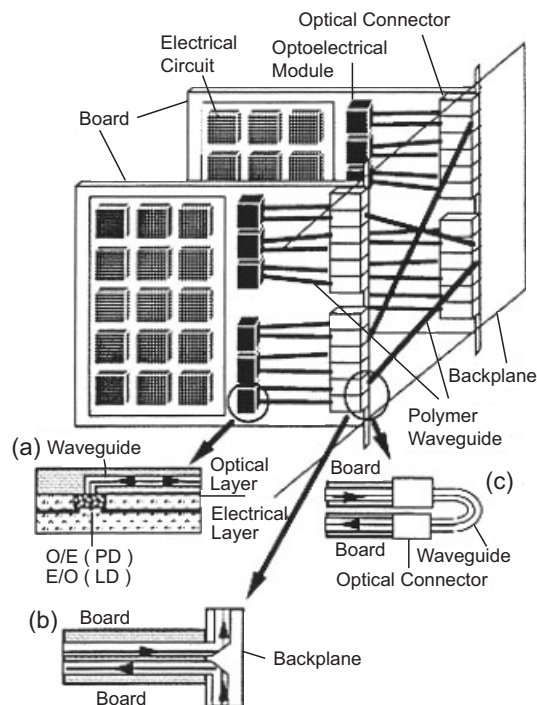


Fig. 4. Schematics of optical interconnects in computing systems. a) 90° out-of plane optical deflector in optical paths between waveguides and electro-optic (E-O)/opto-electronic (O-E) devices such as light-emitting diodes (LEDs) and photodiodes (PDs), b) 90° out-of plane optical deflector in optical paths between boards and a backplane, c) flexible waveguide films where connectors are connected between boards. (Reprinted with permission from [50a]. Copyright 1998, Elsevier Science, New York).

nects in computing systems. Free standing polymeric optical waveguide films with 45° mirrors and MT connectors (mechanically transferable spacing connectors) were fabricated by spin coating, photolithography, and reactive ion etching. The 45° mirror was formed in the waveguide by using a 90° V-shaped diamond blade, and the mirror loss was 0.3–0.7 dB cm<sup>-1</sup> depending on the measurement condition. Free-standing polymeric waveguide films were mounted in an MT-compatible connector made of Pyrex glass by using UV curable resin. The insertion loss was about 1 dB cm<sup>-1</sup>, which was sufficiently low for practical use.

## 4.2. Planar Optical Components for Wavelength Division Multiplexing Telecommunication Systems

### 4.2.1. Splitter, Combiner, and Directional Coupler

The simplest passive optical component is the splitter, a device that distributes optical power incident on the input port into specified power fractions at the output ports.<sup>[51]</sup> A symmetrical 1 × *N* splitter divides the power into *N* ports with a fraction 1/*N* of the incident power each (assuming no other sources of loss). Thus an ideal 1 × 8 splitter, for example, has outputs with power reduced by 9 dB compared to the input power level. In practice, ideal splitters have been demonstrated for some time using fused biconic taper (FBT) fiber technology. However, the drawbacks are the relatively narrow-band performance, vibration sensitivity, and difficulty in scaling to very high port counts. Planar splitters, as realized in silica-on-silicon or polymer waveguides, benefit from ease of fabrication (especially at high port counts) and reduced wavelength dependence, since splits can be based on Y junctions as opposed to extended directional couplers (as in FBT). However, planar splitters generally suffer from increased insertion loss compared to FBT splitters, at least at low port counts, owing to fiber-waveguide coupling loss. Therefore, propagation loss within the planar splitter must be kept to an absolute minimum to remain competitive. As there are no significant performance advantages of polymer technology over planar glass technology for this application, the waveguide losses must be equal to or less than those of planar glass, or on the order of 0.02 dB cm<sup>-1</sup> at 1550 nm.<sup>[15]</sup>

Figure 5 presents an integrated semiconductor four direct feedback (DFB) laser array with a polymer-based 1 × 4 power combiner on the same InP substrate.<sup>[52]</sup> This new approach

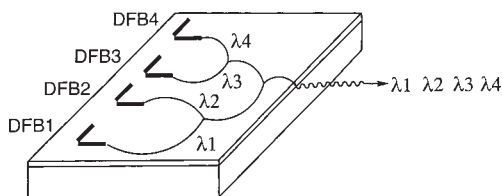


Fig. 5. Polymer waveguide combiners.

brings a number of advantages compared to present purely semiconductor based devices, such as the low polymer waveguide optical losses, the high and easy processability, and the capability of the preparation of polymeric passive components on already processed III–V wafers. A directional coupler is also one of the most important elements in optical integrated circuits.<sup>[53]</sup> It is used for constructing many components, such as power splitters, mux/demuxes, and optical switches.

### 4.2.2. Arrayed Waveguide Grating Multi-/Demultiplexer

Another passive optical component of increasing interest is the arrayed waveguide grating (AWG), a cleverly designed device that uses a concept employed by phased array radar to obtain highly efficient wavelength multiplexing and demultiplexing. A typical *M* × *N* AWG is shown in Figure 6, which il-

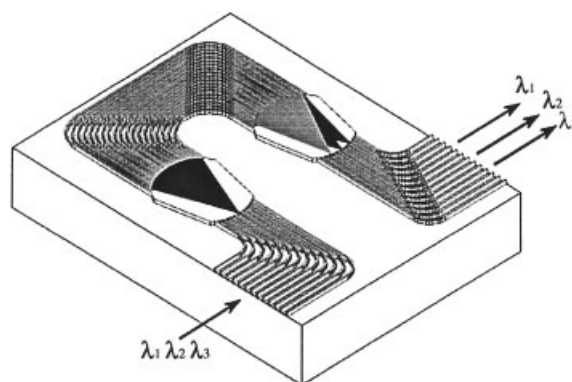


Fig. 6. Array-waveguide grating multiplexer/demultiplexer (contributed by Prof. Y.-J. Ray Chen, UMBC).

lustrates the regions of the device including the inputs, slab regions, phase delay section, and outputs. Planar glass AWGs are already highly successful products used in large volume in optical networks,<sup>[8]</sup> so it would be expected that polymer-based AWGs would have to attain the same performance as silica-based AWGs to achieve acceptance, once again driving interest toward very low loss waveguide materials. An additional requirement for AWGs is that the polarization dependence of the waveguides be very low, so that polarization-dependent losses and polarization-dependent shifts in the filter performance are minimized. One potential advantage of polymer waveguide technology for AWGs is the ability to make completely polymer-based AWGs that are temperature independent, thus potentially requiring no costly and cumbersome temperature control technology, as is generally needed for the planar glass devices.<sup>[54]</sup> By matching the positive coefficient of thermal expansion (CTE) of the polymer substrate and the negative thermo-optic (T-O) coefficient of the waveguide material, the implementation of a polarization-independent and temperature-independent AWG has been demonstrated<sup>[55]</sup> (Figs. 7 and 8).

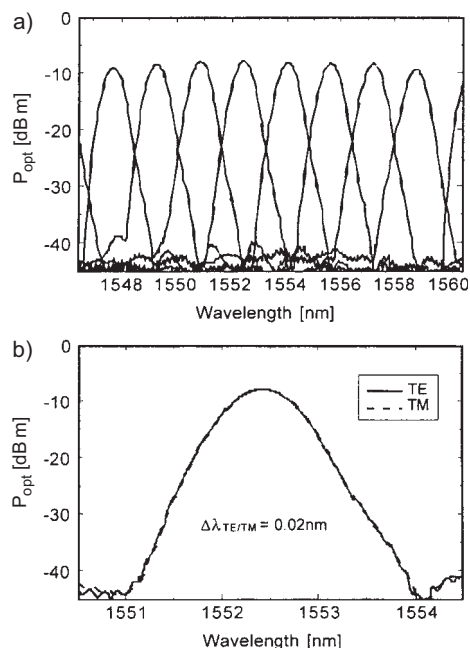


Fig. 7. Measured spectral response (a) and the TE/TM polarization shift (b) of an all-polymer  $8 \times 8$  AWG (200 GHz) wavelength router. (Reprinted with permission from [55]. Copyright 2001, Springer-Verlag, Berlin).

#### 4.2.3. Switches

Modulators and optical switches are two of the most important active components that operate on optical signals

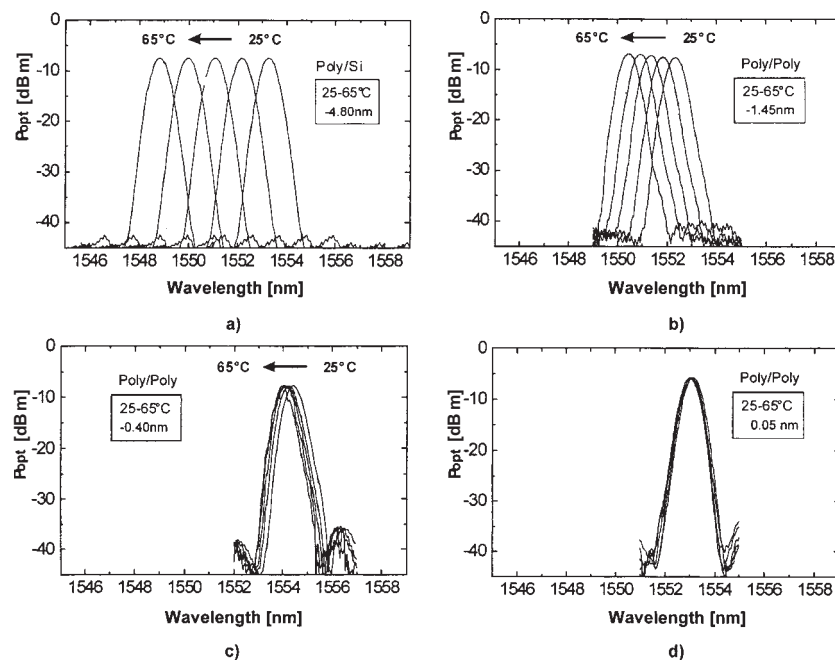


Fig. 8. Measured temperature shift of two different polymer-based  $8 \times 8$  AWGs (200 GHz) in the temperature from 25 °C to 65 °C (in steps of 10 °C). a) On a silicon substrate. b) On polymer substrate A. c) On polymer substrate B. d) On polymer substrate C. (Reprinted with permission from [55]. Copyright 2001, Springer-Verlag, Berlin).

passing through fiber optic systems.<sup>[56]</sup> They are active in two senses: they require external electrical input power and alter the signals in a variable way—functions that are becoming increasingly important as fiber optic systems grow more sophisticated. All-optical networks will require complex optical switches and routers to direct signals to their proper destination. Compared to opto-mechanical switches, waveguide switches including thermo-optic (T-O) and electro-optic (E-O) switches, offer entirely solid-state operation. T-O switches are slower than E-O switches, but they are easier to operate. Their millisecond response times are adequate for most types of optical switching, so they have been more practically applied over times. Another advantage of T-O switches is that they can generally be made to be polarization independent. Meanwhile, electro-optic switches will find their niche in high-speed applications, especially in the military area.

**T-O Switches:** The operating principle of the polymer T-O switch is based on the temperature dependence of the refractive index of the waveguide material. The driving power and the response time of the T-O device depend mainly on the thermal properties (i.e., the thermal conductivity, the temperature coefficient of the refractive indices and the specific heat of the buffer, guiding, and cladding layers and the substrate material, and on the dimensions of the waveguide and heater). Two kinds of polymer waveguide switches, i.e., the interferometric-type switch<sup>[57]</sup> relying on modal interference and the digital optical switches (DOSs)<sup>[58]</sup> relying on adiabatic mode evolution have been investigated. Mach-Zehnder or directional coupler-type switches belong to the group of interferometric-type switches. They show low crosstalk at low switching power but they are wavelength sensitive and the switching power and ambient temperature have to be precisely controlled. An integrated  $4 \times 4$  polymer T-O switch at 1.55  $\mu\text{m}$  is shown in Figure 9. The polarization sensitivity of this device was typically less than 0.5 dB and the response time was less than 1 ms. Its electrical power consumption was found to be 70 mW per single switch. DOSs are rather bulky but they are wavelength insensitive and, thus, there is no need for precise control of switching power and temperature. Recently, DOSs consisting of a symmetrical Y-branch or a symmetric/unsymmetric X-crossing have been demonstrated. The  $1 \times 2$  DOS is considered to have switched once it reaches the desired isolation value, which occurs at some level of electrical power dissipation in the electrodes, beyond which power level the device maintains the isolation, resulting in its well-known “digital” behavior. Any size  $M \times N$  switch can be built out of the combination of several  $1 \times 2$  switches.

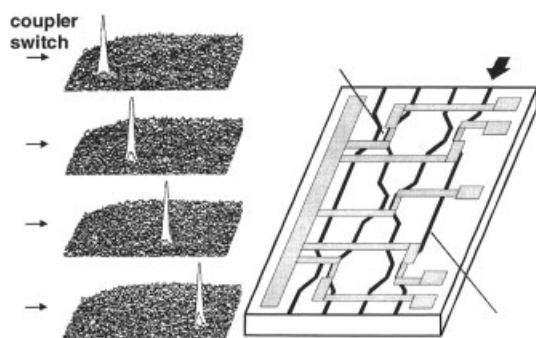


Fig. 9. Schematic layout of a 4×4 polymer T-O switch and near field at 1.55 μm. (Reprinted with permission from [57a]. Copyright 1994, IEEE, Piscataway, NJ).

**E-O Modulators and Switches:** For polymeric E-O materials to be adopted commercially, they must exhibit properties that are competitive with commercial materials such as lithium niobate E-O and gallium arsenide electro-absorptive materials. A well-recognized advantage of polymeric materials is that of bandwidth. The low and relative frequency-independent dielectric constants and refractive indices of organic materials naturally lead to intrinsic material bandwidth on the order of 350 GHz (measured by pulsed techniques for a 1 cm device). Operation of devices fabricated from polymeric materials has been demonstrated to 113 GHz.<sup>[59]</sup> Another putative advantage of polymeric E-O materials, which has recently been mentioned, is that of processibility and ease of integration with disparate materials. Polymeric E-O devices have been successively integrated with VLSI semiconductor electronic circuitry and passive fiber optical circuitry. By using a modified optical push-pull Mach-Zehnder interferometer (MZI) architecture in modulator design (Fig. 10), a half-wave voltage of 0.8 V and a half-wave voltage-interaction length

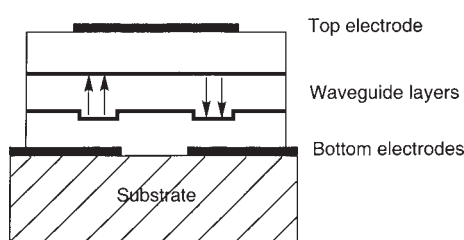


Fig. 10. Operation principle of polymer push-pull E-O modulators. The arrows indicate the molecular alignment directions.

product of 2.2 V cm have been achieved from a guest/host E-O poly(methylmethacrylate) using a high  $\mu\beta$  polyene-type chromophore.<sup>[60]</sup> The push-pull architecture improves the device's modulation efficiency by 6 dB because it can reduce  $V_\pi$  by a factor of 2 when compared with single-arm modulation at the same interaction length. However, materials and device reliability and stability are more challenging since the E-O effect in polymers derives from chromophores that are electrically aligned (poled) in the polymer matrix. By using a constant DC bias to keep the chromophores from orientational relaxation, an  $r_{33}$  as much as three times of the partially re-

laxed residual  $r_{33}$  after poling has recently been observed.<sup>[61,94]</sup> Thus, it also reduces the half-wave voltage due to the utilization of the full potential of E-O polymers. The device based on a constant DC bias was operated as a birefringent modulator (Fig. 11). The temperature of the modulators was maintained by a closed-loop system consisting of a temperature controller, a thermoelectric cooler (TEC), and a thermistor.

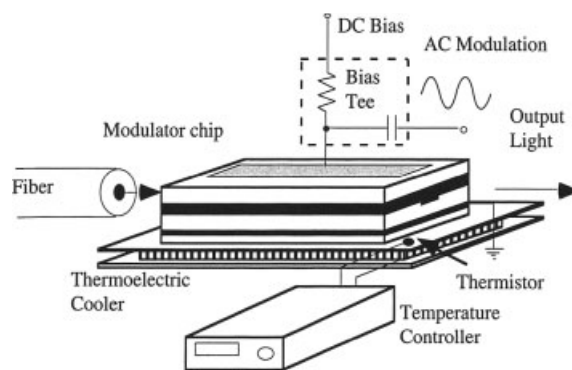


Fig. 11. DC biased E-O polymer waveguide modulators. (Reprinted with permission from [94]. Copyright 1999, Elsevier Science, New York).

The lower electrode was grounded, and a DC bias voltage was applied to the top electrode to create a constant electric field that actively aligns the dipole of the chromophores. The AC modulating voltage was coupled to the top electrode through a bias tee circuit consisting of a capacitor and a resistor. Light of 1.31 μm wavelength was coupled into the optical waveguide from the single-mode fiber pigtail of a 1.4 mW semiconductor laser. However, thus far their polarization-dependent response precludes any actual use in optical telecommunication switching systems. The traditional uniform poling procedure, a pre-requisite processing step for E-O polymer-based devices whereby an electric field is applied at a temperature in the vicinity of the glass-transition temperature, results in uniform statistical polar orientation of the chromophores, and is, therefore, responsible for polarization sensitivity. By means of different coplanar or sandwich electrode configurations, any desired pre-requisite modulation axis can, however, be imprinted onto the material, thus resulting in the possibility of balanced TE/TM polarization efficiencies. Monolithic integration of both electrode configurations with a Mach-Zehnder modulator is shown to result in an original polarization insensitive E-O polymer amplitude modulator for integrated optics (Fig. 12).<sup>[62]</sup> A digital optical modulator based on an asym-

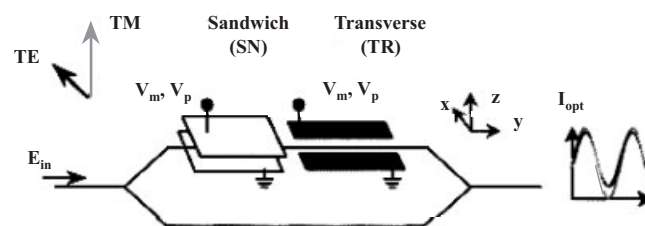


Fig. 12. Polymer-based polarization insensitive amplitude modulators. (Reprinted with permission from [62]. Copyright 2000, Elsevier Science, New York).

metric Y-branch waveguide is proposed and fabricated by using an E-O polymer,<sup>[63]</sup> which shows the potential for polarization- and wavelength-insensitive operation.

Although great progress has been achieved in polymeric E-O modulators, there are only a few reports on polymeric E-O switches:<sup>[64]</sup> the balanced bridge Mach-Zehnder interferometer switch incorporating a 3 dB coupler, the switch consisting of asymmetric Y-junctions and an MZI, and the switch with a modified bifurcation optically active waveguide structure. Figure 13 shows a  $1 \times 4$  integrated electro-optic switch fabricated using a high-temperature E-O polyimide material system, Op-

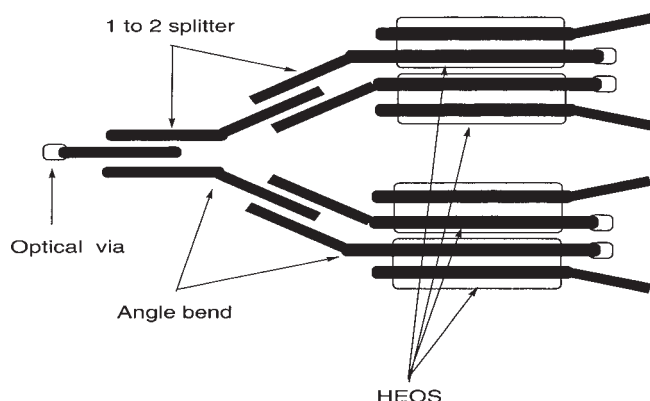


Fig. 13. A  $1 \times 4$  integrated E-O switch using a HEOS.

timer, and a high-temperature electro-optic switch (HEOS) device structure. The switch consists of all the basic circuit elements that are necessary for the fabrication of other E-O devices including optical MCMs. The whole device occupies an area of less than  $0.4 \text{ cm}^2$  so that 122 tiles of them can be fabricated directly on a single 6 in. (1 in.  $\sim 2.5 \text{ cm}$ ) wafer using standard integrated circuit processes. Digital optical switching of this type of device at 2 GHz has been demonstrated with an applied voltage of 10 V.

#### 4.2.4. Tunable Filters

A wavelength tunable filter is an important device for WDM systems because of its multichannel selectivity. The requirements for a practical tunable filter are high wavelength resolution, low polarization-dependence, low levels of crosstalk, and low insertion loss. A polymeric AWG-based thermo-optic tunable filter<sup>[65]</sup> has been recently reported, which was made of cross-linked silicone and operated at around  $1.55 \mu\text{m}$ . This filter exhibited a TE-TM polarization shift of  $< 0.03 \text{ nm}$ , a crosstalk of  $< -35 \text{ dB}$ , an insertion loss of  $< 3 \text{ dB}$ , and a tuning range of  $8.8 \text{ nm}$  in the  $25^\circ\text{C}$ – $75^\circ\text{C}$  temperature region. In addition to this work, two other types of polymeric AWG-based thermo-optic tunable filters<sup>[66]</sup> have also been developed, each with a pair of triangular phase shifters. Both filters operated with a low cross-talk of  $< -25 \text{ dB}$ , one with a tuning range of  $> 30 \text{ nm}$  for a large-scale system and the other with a tuning range of  $\approx 10 \text{ nm}$  for a small-scale system.

Although these results are quite impressive, the performance of AWG-based thermo-optic tunable filters is not as efficient as that of competing technologies such as the fiber Bragg gratings (FBG) or thin film interference filters. However, by combining the advantages of planar devices, such as lithographic manufacturing with a filter performance approaching that of FBGs, photochemically produced Bragg gratings in polymer waveguides have been fabricated. The resulting polymer Bragg gratings (PBGs) have the potential for achieving excellent filter characteristics, relatively low insertion loss through proper integrated optic design, and modularity, a highly valued quality of FBGs. One PBG<sup>[28]</sup> has been tuned by actuating a heater for a polymer with a  $dn/dT$  of  $-3.1 \times 10^{-4}/^\circ\text{C}$  (about 30 times larger than in glass), resulting in a tuning rate of  $-0.36 \text{ nm}/^\circ\text{C}$ , therefore permitting tuning across the entire erbium C-band (1520 to 1565 nm) with a temperature range of about  $100^\circ\text{C}$ .

#### 4.2.5. Variable Optical Attenuator

The variable optical attenuator has attracted extensive attention due to its promising applications in dense wavelength division multiplexing (DWDM) systems. It is used to control the gain of optical amplifiers, thus equalizing the channel powers at add/drop nodes of DWDM systems. It can also dynamically regulate the channel powers regardless of fluctuations in the input light power and polarization. It is expected that an array structure containing multiple attenuators on a single chip is preferable for future DWDM system applications. One of the most critical issues for the implementation of the array is the electrical power consumption of the unit device involved. In this regard, polymer-based T-O variable optical attenuators (VOAs) are quite promising.

VOAs can be based on any switching principle, including interferometry, mode transition, or mode confinement. A low-power consumption T-O VOA that incorporates a membrane-type asymmetric branch waveguide in polymers has been reported.<sup>[67]</sup> The measured electrical power consumption of the attenuator is as small as 25 mW at 1550 nm, which is reduced by about 50 % compared to that of conventional polymer devices. Recently, it has been reported that an 8-channel polymeric VOA array based on MZI exhibits an ultra-low power consumption of about 1.5 mW for 30 dB attenuation.<sup>[28]</sup> Also, a novel VOA based on the Gemfire's leaky mode design has been recently demonstrated with very promising results.

#### 4.2.6. Amplifier

The rapid expansion of optical telecommunication technology also increases the need for planar optical amplifiers that can be used to compensate losses in splitters, multiplexers, switches, and other devices. These losses could be due to imperfections in the waveguide, inefficient coupling and decoupling, mismatch between the laser mode and the waveguide mode, or decrease in the intensity due to splitting of the beam. Planar optical amplifiers<sup>[68]</sup> have been widely studied and use

the rare earth ions erbium or neodymium as the active element because these ions exhibit intra-4f transitions around 1550 nm and 1340 nm, respectively. Amplification is obtained by optical pumping of the rare-earth ions in order to create population inversion. Stimulated emission induced by the signal light then results in optical amplification. An important aspect of polymer-based waveguide amplifiers is the potential for the incorporation of various rare earth species at higher concentrations than can be achieved in inorganic glasses. Since the rare earth is molecularly incorporated, the local environment is better controlled than in the inorganic glass case, further providing for selective codoping of energy transfer agents (such as  $\text{Yb}^{3+}$  for  $\text{Er}^{3+}$ )

There are two kinds of approaches, butt-end coupling and distributed coupling, to realize the pumping of an optical waveguide amplifier. Butt-end coupling is done by coupling the pump beam into the waveguide at the input facet of the waveguide. The pump light is absorbed by the rare-earth ions as it travels through the waveguide, resulting in a decrease in pump power along the waveguide. In order to maintain sufficient pump power over the entire length of the waveguide, relatively high pump powers are coupled into the input section of the waveguide. This pumping scheme can be successfully used for materials in which high pump powers do not affect the pumping efficiency. However, in several materials systems, an optimum pump power for amplification exists. Such systems include Er-doped waveguides in which cooperative up-conversion and excited-state absorption take place, or systems in which the rare-earth ions are excited via an energy transfer from a sensitizer. In these systems, butt-end coupling is not efficient. The excess pump power at the beginning of the waveguide will result in pump absorption, which does not contribute to the optical gain.

Distributed coupling is based on the coupling between two adjacent waveguides, where pump light is gradually coupled from a non-absorbing pump waveguide into the amplifier waveguide. The coupling between the waveguides in such a configuration is calculated using an improved coupled mode theory (CMT). The proposed distributed coupling scheme can enhance the optical gain in systems that exhibit a reduced pump efficiency at high pump power. An example of this enhancement has been shown for a sensitized neodymium-doped polymer waveguide amplifier,<sup>[69]</sup> in which the optical gain increases from 0.005 dB to 1.6 dB by changing from the conventional butt-coupling to the distributed coupling.

### 4.3. Planar Optical Waveguides for Sensors

Several topics in optical sensors have evoked significant commercial interest including: light emission from labeled fluorophores, absorption spectroscopy, and surface plasmon resonance (SPR) from both bulk prisms and planar optical waveguides. Optical waveguide formats offer a more flexible option over bulk optical systems, to fabricate a compact, disposable, and integrated sensor with an appropriate waveguide

structure and wide tolerance in applications. Planar optical waveguides are very sensitive to changes in parameters such as refractive index, absorption and emission spectra due to temperature, humidity, pressure, and chemical species. Parameter changes cause modulation of light traveling within the optical waveguides, and is useful for optical sensing in industrial, environmental, medical, civilian, and military applications. A planar geometry utilizing waveguide-coupled SPR<sup>[70]</sup> may have a theoretical sensitivity of  $\Delta n = 2 \times 10^{-5}$ . Grating structures in planar waveguides,<sup>[71]</sup> coated with thin, highly specific, and responsive chemical coatings that can respond to sub-monolayer film formation by adsorption or binding of antibody molecules within seconds with a theoretical minimum index change of  $\Delta n = 2 \times 10^{-6}$  have been developed for biochemical sensors. A Mach-Zehnder interferometer has been used to detect antibodies absorbed onto waveguide surfaces at a concentration of  $5 \times 10^{-11}$  M HCG (human chorionic gonadotropin) at  $2.5 \text{ ng mL}^{-1}$  in 20 min.<sup>[72]</sup>

Recently, polymer-based optical waveguide sensors have been explored because in inorganic waveguide systems it is difficult to control stress, refractive index, and uniformity. By using polymer-based waveguide systems, optical sensors have been achieved with small residual stress, easy fabrication, and low cost. For an optomechanical pressure sensor using polymer multi-mode interference couplers, a high sensitivity of 8.2 ppm/Pa has been obtained.<sup>[73]</sup> Sensitivity of several parts per million humidity concentrations have also been achieved for a polymer waveguide sensor with a symmetric multilayer configuration.<sup>[74]</sup>

### 4.4. Integrated Planar Lightwave Circuits

To fully realize the function of polymer optical waveguide devices, the integration of light sources, optical transmission waveguides, optical components, and optical sensors/detectors are necessary. On the other hand, the performance of optical components can also be enhanced by their integration. Recently, several kinds of integrated planar lightwave circuits have been fabricated.

#### 4.4.1. Tunable Optical Add/Drop Multiplexers

The fabrication of Bragg-grating-based multichannel optical add/drop multiplexers in polymers has been reported.<sup>[75]</sup> These filters are designed by cascading multiple stages of single-channel mux/demuxes. Each stage consists of a Mach-Zehnder interferometer (MZI) with a Bragg grating across its arms. The 3 dB couplers in each MZI are multi-mode interference (MMI) couplers, which offer excellent tolerance to polarization and wavelength variation, and relaxed fabrication requirements compared to alternatives such as directional couplers, adiabatic X- or Y-junctions, and diffractive star couplers. The gratings were printed photochemically, achieving index differences as high as  $10^{-3}$  and reflectivities as large as 33 dB. The 3D bandwidth is about 0.2 nm. Anodization is

used to reduce side lobes in the reflection spectrum. The Bragg gratings in the four MZIs have slightly different periods (Fig. 14a). The grating closest to the input port reflects at wavelength  $\lambda_1$ , so light at that wavelength launched at the in-

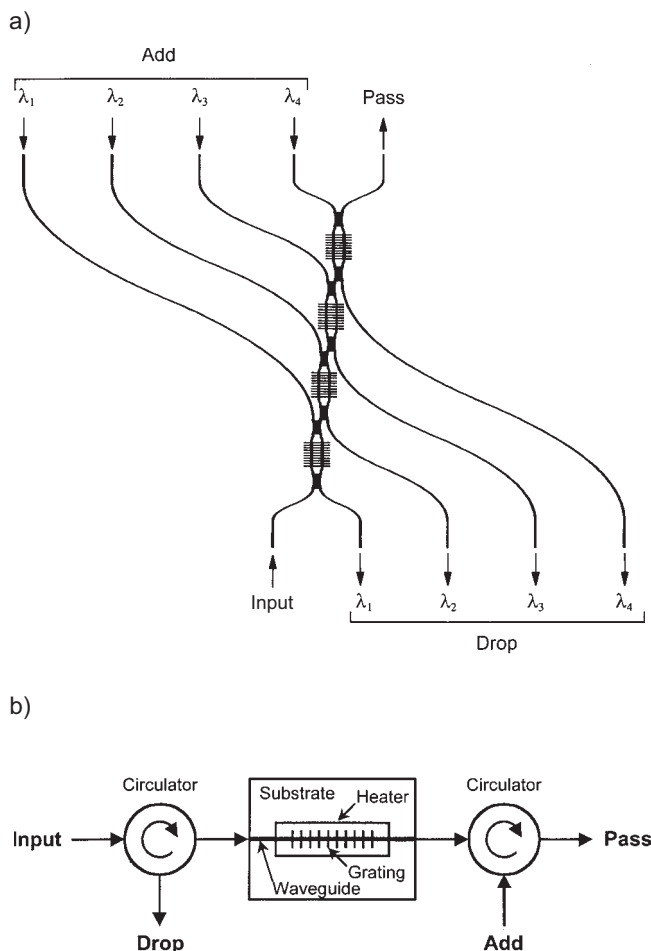


Fig. 14. Tunable optical add/drop multiplexers (OADMs). (Reprinted with permission from [75], [76]. Copyright 1998 and 1999, IEEE, Piscataway, NJ).

put port exits the drop port labeled  $\lambda_1$  while light at that wavelength launched into the add port labeled  $\lambda_1$  exits the pass port. The resulting four-channel optical add/drop multiplexers (OADMs) exhibit the proper 400 GHz channel separation and International Telecommunications Union (ITU) grid wavelength alignment, as well as excellent channel isolation and uniform channel response.

Another way to form an OADM is to place a grating between optical circulators.<sup>[76]</sup> In the past, an OADM has been implemented with fiber Bragg gratings, however due to the small  $dn/dT$  of glass, the filters cannot be tuned thermally, and must be tuned by less reliable mechanical means. Tunable OADM can be achieved by combining thermally tunable planar polymer Bragg gratings with optical circulators (Fig. 14b). The grating exhibits better than 45 dB reflection with no detectable out-of-band reflection. These OADM have a high-bandwidth utilization factor of 0.92, with a minimum channel spacing of 75 GHz. They are tunable at a rate

of  $-0.256 \text{ nm}/^\circ\text{C}$ . Tuning over a 20 nm range has been demonstrated with a single device.

#### 4.4.2. Photonic Crystal Superprism Waveguide

Photonic crystals (PCs) are artificial structures, which have a periodic dielectric structure with high index contrast, designed to control photons in the same way that conventional crystals in solids control electrons. Extensive efforts have been made to find structures that completely forbid propagation of photons within a certain range of energies called a photonic bandgap.<sup>[77]</sup> Also, the energy dispersion called a photonic band structure has shown a number of interesting phenomena.<sup>[78]</sup> Photonic crystals have very large dispersion characteristics (500 times that of a regular prism and more than 50 times stronger than that of a conventional grating), which makes them very attractive for WDM applications.<sup>[79]</sup> Using polymer waveguide technology and block copolymer photonic bandgap materials, it is possible to fabricate a waveguide superprism within polymeric planar waveguide circuits. New optical devices and the miniaturization of current integrated optical devices may result. A simple integrated WDM demultiplexer circuit can be fabricated from a quadrilateral 2D photonic crystal element.<sup>[80]</sup> This integrated optical demultiplexer reduces component size by hundreds of times compared to conventional devices. Significantly, there is no restriction on the free-spectral range caused by the high-order diffraction in the demultiplexer based on a conventional grating.

#### 4.4.3. Digital Optical Switches with Variable Optical Attenuators

Digital optical switches (DOSs), which have been realized using different materials, show a crosstalk (CT) of about  $-20 \text{ dB}$ , which is still insufficient for network applications. An improved CT value was achieved with a W-shaped DOS or a cascade of DOSs and attenuator. Recently, a polymer DOS with an integrated attenuator<sup>[81]</sup> (Fig. 15) showed a crosstalk

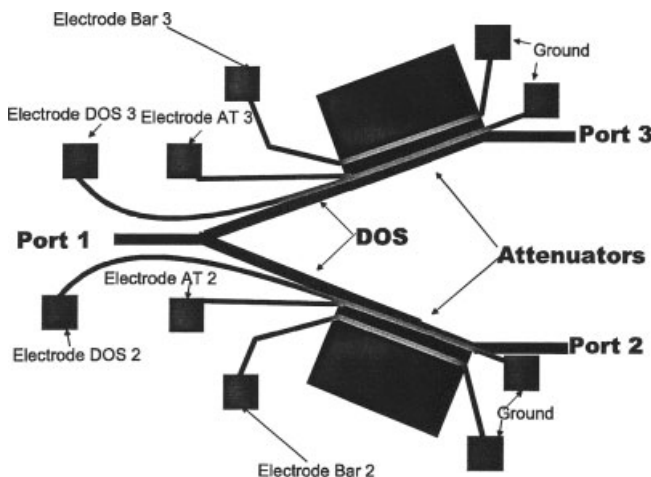


Fig. 15. DOS with integrated attenuator and electrodes. (Reprinted with permission from [81]. Copyright 2001, IEEE, Piscataway, NJ).

value of  $-46$  dB, but the higher power consumption and the additional insertion losses need to be reduced. Based on Y-branched wide-angle DOSs, a polymer  $1 \times 2$  DOS integrated with a VOA<sup>[82]</sup> showed low switching power without adversely affecting the crosstalk. This switch exhibited a low crosstalk value of about  $-40$  dB, and the switching power was  $\approx 170$  mW at  $1.55$   $\mu\text{m}$ .

#### 4.4.4. Light-Emitting Diodes for Polymer Optical Waveguides

Organic light-emitting diodes (OLEDs) utilizing fluorescent dyes or conjugated polymers have attracted great interest because they are capable of emitting light that can cover almost the whole visible spectral range and are highly efficient, requiring only a quite low driving voltage ( $2\text{--}10$  V).<sup>[83]</sup> Recently, OLEDs have also been demonstrated to have a long lifetime ( $> 20\,000$  h) and excellent durability for flat-panel display applications. An additional advantage is that they are simple to fabricate on various kinds of substrates, including polymer and glass substrates. The combination of polymer waveguides and organic optical devices<sup>[84]</sup> will provide huge advantages for fabricating optical integrated circuits such as is shown in Figure 16. The organic electroluminescent (EL) device was fabricated on a polymer waveguide with Alq<sub>3</sub> as the

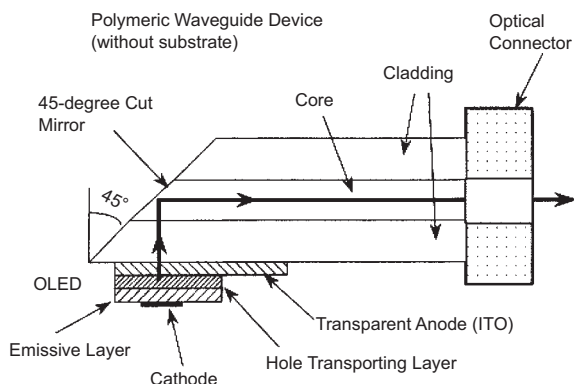


Fig. 16. An integrated organic light-emitting diode with a polymeric waveguide device. (Reprinted with permission from [84]. Copyright 2001, Elsevier Science, New York).

light-emitting material and *N,N'*-diphenyl-*N,N'*-bis(3-methylphenyl)-(1,1'-biphenyl)-4,4'-diamine (TPD) as the hole-transporting material. The transmission loss was estimated to be  $1.35$  dB  $\text{cm}^{-1}$  at  $520$  nm with the light from the OLED. Optical pulses of faster than  $5$  Mb  $\text{s}^{-1}$  (Mb = megabytes) were generated by directly modulating the OLED. Since polymer waveguides have a low transmission loss in the near-infrared and red light region, use of light-emitting devices at these wavelengths will provide an efficient tool for optical integration.

#### 4.4.5. Traveling-Wave Heterojunction Phototransistors

Although much work has been done on high-speed phototransistors,<sup>[85]</sup> a classic design conflict exists between the simultaneous optimization of high-frequency performance and

optical coupling efficiency. In lumped-element heterojunction phototransistors (HPTs), the devices need to be scaled down in size for high-speed operation. These small devices tend to saturate at low input optical power levels because of the absorption volume. Traveling-wave (TW) concepts have been implemented successfully in optical modulation technology. By extending these concepts to HPT detectors, a schematic diagram of a TW-HPT<sup>[86]</sup> is shown in Figure 17. In this approach, a leaky-mode polyimide waveguide on top of the active region of the HPT is defined. Intensity-modulated light is coupled to the polyimide waveguide and leaks into the HPT's

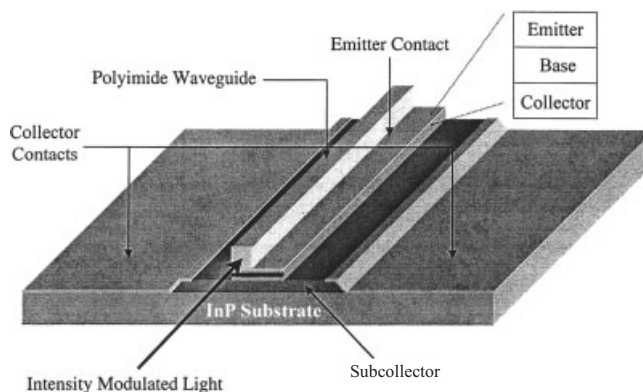


Fig. 17. Traveling-wave heterojunction phototransistors. (Reprinted with permission from [86]. Copyright 1998, IEEE, Piscataway, NJ).

active region along the length of the device due to the fact that the refractive index of the semiconductor is higher than that of the polyimide. The metal pads of the HPT are coplanar waveguides with the center line contacting the emitter and the ground plane contacting the collector. The base is floating. The ultimate bandwidth limitation of such a device is based on the velocity mismatch between the optical wave and the induced electrical microwave.<sup>[87]</sup> Due to the integration of the polyimide waveguide and the HPT in the TW configuration, power saturation effects are improved because the absorption of the incident light signal is distributed along the entire length of the device. High optical gain with an input optical coupling efficiency of  $70\%$  was demonstrated. A  $200$   $\mu\text{m}$  long TW-HPT also exhibited no output power saturation up to  $50$  mA of DC photocurrent at an operating frequency of  $60$  GHz.

#### 4.5. Vertical Integration and 3D Integrated Optics

Conventional two-dimensional (2D) guided-wave integrated optics provides a reliable and structurally stable method for interconnecting optical devices in photonic circuits and for the optical interconnection of high-density integrated electronics. However, in two dimensions, the complexity of the photonic circuits is limited by the size of the substrate and by the difficulty of connecting a large number of input and output fibers or electrical connections. The possibility of adding the third dimension to integrated optics would greatly in-

crease the integration density and would overcome some of the input–output problems while preserving the reliability and structural stability of guided wave optics. Three-dimensional (3D) integrated optics consists of vertically stacked layers of horizontal 2D integrated optics with properly placed vertical waveguide interconnects between the layers. For 3D optical integration, optical polymers have some significant advantages over other materials such as semiconductors or silica. The vertical features of optical polymers can be etched by using shadow mask etching or a photoresist as the etch mask. In addition, optical polymers can have excellent adhesion to a number of surfaces, and, by varying the doping level or by combining multiple polymer systems, precise control of the index of refraction is possible. Recently, a series of vertical waveguide bends,<sup>[88]</sup> waveguide power splitters,<sup>[88]</sup> waveguide polarization splitters,<sup>[89]</sup> and coupler switches<sup>[90]</sup> have been fabricated based on optical polymers. Moreover, 3D integrated Mach-Zehnder modulators,<sup>[91]</sup> directional couplers,<sup>[92]</sup> optical fan-out devices,<sup>[93]</sup> and E-O devices<sup>[88,94]</sup> have also been realized in polymer material systems.

Vertical polarization splitters split the polarization vertically into two different levels of stacked 2D integrated optical circuits. Vertical polarization splitters and the concept of 3D integrated optics may have particular application in polarization diversity systems in which polarization insensitivity is achieved by providing two identical processing channels; one of each orthogonal polarization. In this approach, the two signal processing circuits are stacked vertically, and the vertical polarization splitter separates the random input polarization between the layers. A vertical polarization splitter<sup>[89]</sup> (Fig. 18) based on birefringent polymers yielded extinction ratios as high as 22 and 12 dB for TE and TM polarization, respectively.

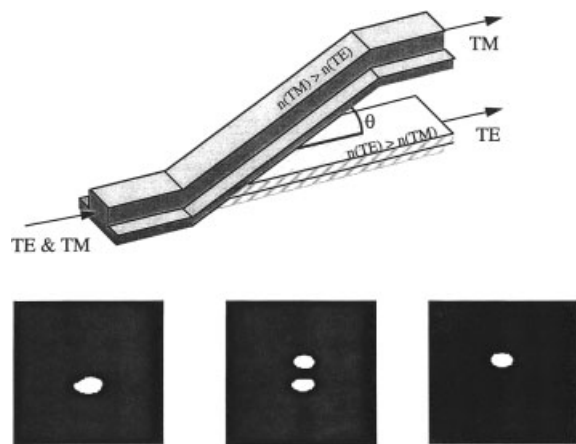


Fig. 18. Fabricated polymer vertical polarization splitter. (Reprinted with permission from [89]. Copyright 1999, IEEE).

The schematic layout of a  $1 \times 2$  vertical coupler switch (VCS)<sup>[90]</sup> with three vertical switching elements, along with the cross section of the polymer/silica layer structure is shown in Figure 19. It can be seen from the cross section that the  $1 \times 2$  VCS has a vertical stack structure comprising a silica

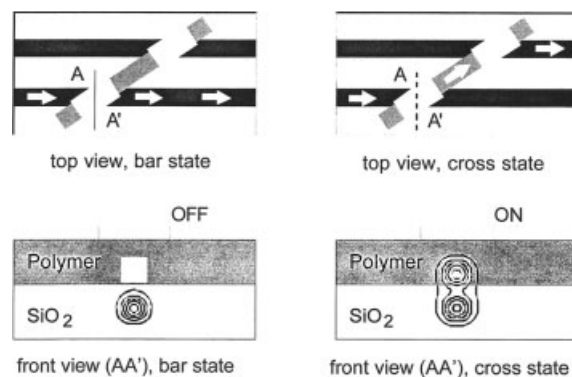


Fig. 19.  $1 \times 2$  polymer/silica vertical coupler switches and field distribution. (Reprinted with permission from [90]. Copyright 2001, Springer-Verlag, Berlin).

guiding layer, a gap layer, a polymer waveguide, and a heating electrode. In this VCS, the  $\text{SiO}_2$  waveguide is only used as an optical transmission layer, and the planar polymer waveguide for the switching function. When all the electrodes are sufficiently powered (ON) the input light is coupled to the polymer waveguide in the first vertical coupler (VC1) and coupled back to an adjacent parallel silica waveguide in the second vertical coupler (VC2). The third switching element (VC3) serves to absorb residual light in the lower silica waveguide to reduce the crosstalk. A hybrid polymer/silica  $1 \times 2$  vertical switch with a polymer gap layer instead of a silica one and with a refractive index contrast of 0.008 has been fabricated to exhibit low insertion loss (1.5 dB), low crosstalk ( $< -32$  dB), low switching power ( $< 80$  mW), and polarization insensitivity. Using this  $1 \times 2$  VCS as a building block, a hybrid polymer/silica  $1 \times 8$  VCS matrix has been realized.

As a 3D integration example, a polymer E-O modulator integrated on top of a passive waveguide<sup>[88,94]</sup> is shown in Figure 20. In this approach, the interconnect waveguide pattern

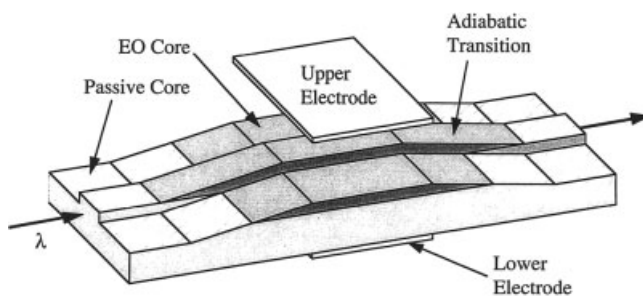


Fig. 20. Polymer E-O modulator integrated on top of low-loss passive polymer waveguide. (Reprinted with permission from [88]. Copyright 1999, IEEE, Piscataway, NJ).

was first fabricated in a low-loss passive polymer system. The active polymer was then placed on top of this layer and patterned into the area where needed. Vertical coupling structures were then fabricated to channel the light up into the passive waveguides. It has been demonstrated that the light coupled almost entirely up into the E-O polymer and down again, and the loss in the transition region was  $\approx 1$  dB.

## 5. Summary and Outlook

From materials to processing to devices, polymer optical waveguides have shown great promise for integrated optical circuits due to their processibility and integration advantages. These advantages also make them an ideal integration platform where foreign material systems, such as lithium niobate, and semiconductor devices, such as lasers, detectors, amplifiers, and logic circuits, can be inserted into an etched groove in a planar lightwave circuit to enable full amplifier modules or optical add/drop multiplexers on a single substrate. Moreover, the combination of flexibility and toughness in optical polymers makes them suitable for vertical integration to realize 3D and even all-polymer integrated optics. Due to the capability of being produced in large volumes at low costs, polymer optical waveguide devices will play a major role in broadband communications, in areas such as optical networking based on dense wavelength division multiplexing metro/access communications, and on computing systems.

However, integrated optics, especially polymer-based integrated optics, is still in its early stage compared to well-established integrated electronics. Optical polymers must meet Telcordia telecom and 25 other essential technical requirements before they can be considered seriously as a viable technology for carrier-class applications. Highly integrated polymer optical waveguide components and circuits also need to demonstrate their full advantages such as size reduction, low cost, performance improvement, higher yields, and shorter time to market.

As a result, the optimization of polymer planar optical components, the integration of polymer passive and active optical waveguide devices, the integration of light sources, optical transmission waveguides, optical components and optical sensors/detectors, and even all-polymer integrated optical circuits will grow. In addition, the introduction of photonic bandgap materials and nanolithographic processing to polymer passive or active optical waveguide devices will present great opportunities for enhancing the performance of polymer-based integrated optics.

Received: July 1, 2002

- [1] a) L. Eldada, *Opt. Eng.* **2001**, *40*, 1165. b) *Design, Manufacturing, and Testing of Planar Optical Waveguide Devices* (Ed: R. A. Norwood), Vol. 4439, SPIE, Bellingham, WA **2001**. c) *Electrical, Optical, and Magnetic Properties of Organic Solid-State Materials V* (Eds: S. Ermer, J. R. Reynolds, J. W. Perry, A. K.-Y. Jen, Z. Bao), Vol. 598, Materials Research Society, Pittsburgh, PA **2000**. d) *Polymer Photonic Devices* (Eds: B. Kippelen, D. D. C. Bradley), Vol. 3281, SPIE, Bellingham, MA **1998**. e) A. J. Heeger, *Angew. Chem. Int. Ed.* **2001**, *40*, 2591.
- [2] a) *Optical Materials* (Ed: R. M. Wood), Cambridge University Press, Cambridge, UK **1993**. b) *Optical Materials* (Ed: S. Musikant), Marcel Dekker, New York **1985**.
- [3] a) *Planar Optical Waveguides and Fibres* (Ed: H. G. Unger), Clarendon Press, Oxford, UK **1977**. b) *Optical Waveguide Concepts* (Ed: C. Vassallo), Elsevier, New York **1991**.
- [4] M. G. Mogul, D. L. Wise, J. D. Gresser, D. J. Trentolo, G. E. Wnek, C. A. Dimarzio, *Photonic Polymer Systems* (Eds: D. L. Wise, G. E. Wnek, D. J. Trentolo, T. M. Cooper, J. D. Gresser), Marcel Dekker, New York **1998**, p. 517.
- [5] a) J. Hecht, *Laser Focus World* **2001**, January, 115. b) J. Hecht, *Laser Focus World* **2001**, October, 69.
- [6] *Optoelectronic Interconnects and Packaging* (Ed: R. T. Chen, P. S. Guilfoyle), Vol. CR 62, SPIE, Bellingham, MA **1996**.
- [7] L. Gasman, *WDM Solutions* **2001**, November, 17.
- [8] a) F. Lipscomb, A. J. Ticknor, M. Stiller, W. J. Chen, P. Schroeter, in *Design, Manufacturing, and Testing of Planar Optical Waveguide Devices* (Ed: R. A. Norwood), Vol. 4439, SPIE, Bellingham, MA **2001**, p. 10. b) T. Maruno, N. Ooba, S. Toyoda, in *Design, Manufacturing, and Testing of Planar Optical Waveguide Devices* (Ed: R. A. Norwood), Vol. 4439, SPIE, Bellingham, MA **2001**, p. 63.
- [9] a) *Polymers for Electronic and Photonic Applications* (Ed: C. P. Wong), Academic Press, New York **1993**. b) *Polymers for Lightwave and Integrated Optics* (Ed: L. A. Hornak), Marcel Dekker, New York **1992**. c) *Photonic Polymer Systems* (Eds: D. L. Wise, G. E. Wnek, D. J. Trentolo, T. M. Cooper, J. D. Gresser), Marcel Dekker, New York **1998**. d) L. Eldada, *IEEE J. Sel. Top. Quantum Electron.* **2000**, *6*, 54. e) H. H. Yao, N. Keil, C. Zawadzki, J. Bauer, M. Bauer, C. Dreyer, in *Design, Manufacturing, and Testing of Planar Optical Waveguide Devices* (Ed: R. A. Norwood), Vol. 4439, SPIE, Bellingham, MA **2001**, p. 36. f) R. A. Norwood, R. Blomquist, L. Eldada, C. Glass, C. Poga, L. W. Shacklette, B. Xu, S. Yin, J. T. Yardley, *Proc. SPIE-Int. Soc. Opt. Eng.* **1998**, *3281*, 2. g) L. Robitaille, C. L. Callender, J. P. Noad, *Proc. SPIE-Int. Soc. Opt. Eng.* **1998**, *3281*, 14. h) L. Dalton, *Adv. Polym. Sci.* **2002**, *158*, 1.
- [10] a) G. Hougham, G. Tesoro, A. Viehbeck, J. D. Chapple-Sokol, *Macromolecules* **1994**, *27*, 5964. b) G. Hougham, G. Tesoro, A. Viehbeck, *Macromolecules* **1996**, *29*, 3453.
- [11] a) S. Herminghaus, D. Boese, D. Y. Yoon, B. A. Smith, *Appl. Phys. Lett.* **1991**, *58*, 1043. b) D. Boese, H. Lee, D. Y. Yoon, J. D. Swalen, J. F. Rabolt, *J. Polym. Sci. Polym. Phys.* **1992**, *30*, 1321.
- [12] M. Kihara, S. Nagasawa, T. Tanifuji, *J. Lightwave Technol.* **1996**, *14*, 1986.
- [13] T. Watanabe, N. Ooba, Y. Hida, M. Hikita, *Appl. Phys. Lett.* **1998**, *72*, 1533.
- [14] L. Eldada, S. Yin, R. A. Norwood, J. T. Yardley, *Proc. SPIE-Int. Soc. Opt. Eng.* **1997**, *3234*, 161.
- [15] R. A. Norwood, R. Y. Gao, J. Sharma, C. C. Teng, in *Design, Manufacturing, and Testing of Planar Optical Waveguide Devices* (Ed: R. A. Norwood), Vol. 4439, SPIE, Bellingham, MA **2001**, p. 19.
- [16] a) A. Skumanich, C. R. Moylan, *Chem. Phys. Lett.* **1990**, *174*, 139. b) W. Groh, *Makromol. Chem.* **1988**, *189*, 2861.
- [17] W. B. Jackson, N. M. Amer, A. C. Boccara, D. Fournier, *Appl. Opt.* **1981**, *20*, 1333.
- [18] C. C. Teng, *Appl. Opt.* **1993**, *32*, 1051.
- [19] *Generic Requirements for Fiber Optic Branching Components*, Bellcore GR-1209-CORE, Bellcore, NJ **1994**.
- [20] *Generic Reliability Assurance Requirements for Fiber Optic Branching Components*, Bellcore GR-1221-CORE, Bellcore, NJ **1994**.
- [21] J. H. Harris, R. Shubert, J. N. Polky, *J. Opt. Soc. Am.* **1970**, *60*, 1007.
- [22] a) M. Kagami, H. Ito, T. Ichikawa, S. Kato, M. Matsuda, N. Takahashi, *Appl. Opt.* **1995**, 1041. b) J. P. D. Cook, G. O. Este, F. R. Shepherd, W. D. Westwood, J. Arrington, W. Moyer, J. Nurse, S. Powell, *Appl. Opt.* **1998**, *37*, 1220. c) R. Schriever, H. Franke, H. G. Festl, E. Kratzig, *Polymer* **1985**, *26*, 1425.
- [23] H. Gokan, S. Esho, Y. Ohnishi, *J. Electrochem. Soc.* **1982**, *1*, 205.
- [24] a) S. Singh, A. Kapoor, S. C. K. Misra, K. N. Tripathi, *Solid State Commun.* **1996**, *100*, 503. b) J. W. Kang, J. S. Kim, J. J. Kim, *Jpn. J. Appl. Phys.* **2001**, *40(5A)*, 3215.
- [25] D. A. Ramey, *IEEE Trans. Circuits Syst.* **1979**, *26*, 1041.
- [26] M. Hikita, R. Yoshimura, M. Usui, S. Tomaru, S. Imamura, *Thin Solid Films* **1998**, *331*, 303.
- [27] a) K. H. Losch, P. Kersten, W. Wischmann, in *Optical Waveguide Materials* (Eds: M. M. Broer, G. H. Sigel, Jr., R. T. Kersten, H. Kawazoe), Vol. 244, Materials Research Society, Pittsburgh, PA **1992**, p. 253. b) R. Ulrich, H. P. Weber, *Appl. Opt.* **1972**, *11*, 428.
- [28] L. Eldada, *WDM Solutions* **2002**, April, 21.
- [29] a) B. L. Booth, *J. Lightwave Technol.* **1989**, *7*, 1445. b) L. W. Shacklette, R. A. Norwood, L. Eldada, C. Glass, D. Nguyen, C. Poga, B. P. Xu, S. Yin, J. T. Yardley, *Proc. SPIE-Int. Soc. Opt. Eng.* **1997**, *3147*, 222. c) L. Eldada, K. M. T. Stengel, L. W. Shacklette, R. A. Norwood, C. Z. Xu, C. J. Wu, J. T. Yardley, *Proc. SPIE-Int. Soc. Opt. Eng.* **1997**, *3006*, 344. d) R. Yoshimura, M. Hikita, S. Tomaru, S. Imamura, *J. Lightwave Technol.* **1998**, *16*, 1030. e) S. Imamura, R. Yoshimura, T. Izawa, *Electron. Lett.* **1991**, *27*, 1342.
- [30] a) K. D. Singer, T. C. Kowalczyk, A. J. Beuhler, in *Sol-Gel and Polymer Photonic Devices* (Eds: M. P. Andrews, S. I. Najafi), Vol. CR 68, SPIE, Bellingham, MA **1997**, p. 399. b) Y. S. Liu, R. J. Wojnarowski, W. A. Hennessey, in *Optoelectronic Interconnects and Packaging* (Eds: R. T. Chen, P. S. Guilfoyle), Vol. CR 62, SPIE, Bellingham, MA **1996**, p. 405. c) T. Matsura, S. Ando, S. Sasaki, F. Yamamoto, *Electron. Lett.* **1993**, *29*, 269. d) J.

- Kobayashi, Y. Inoue, T. Matsuura, T. Maruno, *Denshi Joho Tsushin Gak-kai Ronbunshi, C: Erekutoronikusu (in Japanese) [Trans. IEICE, C]* **1998**, E81, 1020. e) J. Kobayashi, T. Matsuura, S. Sasaki, T. Maruno, *Appl. Opt.* **1998**, 37, 1032. f) T. Matsuura, J. Kobayashi, S. Ando, T. Maruno, S. Sasaki, F. Yamamoto, *Appl. Opt.* **1999**, 38, 966.
- [31] a) G. Fischbeck, R. Moosburger, C. Kostorzewa, A. Achen, K. Petermann, *Electron. Lett.* **1997**, 33, 518. b) D. W. Smith, Jr., S. M. Kumar, S. R. Chen, J. M. Ballato, E. J. Nelson, J. J. Jin, S. H. Foulger, in *Design, Manufacturing, and Testing of Planar Optical Waveguide Devices* (Ed: R. A. Norwood), Vol. 4439, SPIE, Bellingham, MA **2001**, p. 51. c) W. S. Choi, F. W. Harris, *Polymer* **2000**, 41, 6213. d) J. Jin, M. S. Kumar, S. H. Foulger, D. W. Smith, Jr., H. B. Liu, B. Mojazza, P. Go, A. Shep, *Polym. Prepr.* **2002**, 43(1), 609. d) S. E. Lee, D. S. Lee, C. E. Kim, D. K. Yi, M. J. Kim, B. G. Shin, J. W. Kang, J. J. Kim, D. Y. Kim, *Polym. Prepr.* **2002**, 43(1), 625. e) H. Ma, S. Wong, J. D. Luo, S. H. Kang, A. K.-Y. Jen, R. Barto, C. W. Frank, *Polym. Prepr.* **2002**, 43(2), 493.
- [32] a) S. R. Marder, B. Kippelen, A. K.-Y. Jen, N. Peyghambarian, *Nature* **1997**, 388, 845. b) L. R. Dalton, W. H. Steier, B. H. Robinson, C. Zhang, A. Ren, S. Garner, A. T. Chen, T. Londergan, L. Irwin, B. Carlson, L. Fifield, G. Phelan, C. Kincaid, J. Amend, A. K.-Y. Jen, *J. Mater. Chem.* **1999**, 9, 1905. c) H. Ma, S. Liu, J. D. Luo, S. Suresh, L. Liu, S. H. Kang, M. Haller, T. Sassa, A. K.-Y. Jen, L. R. Dalton, *Adv. Funct. Mater.* **2002**, 12, 565. d) Y. Q. Shi, C. Zhang, H. Zhang, J. H. Bechtel, L. R. Dalton, B. H. Robinson, W. H. Steier, *Science* **2000**, 288, 119. e) H. Ma, B. Q. Chen, T. Sassa, L. R. Dalton, A. K.-Y. Jen, *J. Am. Chem. Soc.* **2001**, 123, 986. f) H. Ma, A. K.-Y. Jen, *Adv. Mater.* **2001**, 13, 1201. g) M. E. van der Boom, A. G. Richter, J. E. Malinsky, P. A. Lee, N. R. Armstrong, P. Dutta, T. J. Marks, *Chem. Mater.* **2001**, 13, 15. h) D. R. Kanis, M. A. Ratner, T. J. Marks, *Chem. Rev.* **1994**, 94, 195. i) D. M. Burland, R. D. Miller, C. A. Walsh, *Chem. Rev.* **1994**, 94, 31. j) F. Ghebremichael, M. G. Kuzyk, H. S. Lackritz, *Prog. Polym. Sci.* **1997**, 22, 1147. k) C. Samyn, T. Verbiest, A. Persoons, *Macromol. Rapid Commun.* **2000**, 21, 1. l) J. W. Wu, J. F. Valley, S. Ermer, E. S. Binkley, J. T. Kenney, G. F. Lipscomb, R. Lytel, *Appl. Phys. Lett.* **1991**, 58, 225. m) A. K.-Y. Jen, K.-Y. Wong, V. P. Rao, K. Drost, Y. M. Cai, *J. Electron. Mater.* **1994**, 23, 653. n) Y. M. Cai, A. K.-Y. Jen, *Appl. Phys. Lett.* **1995**, 117, 7295.
- [33] C. F. Kane, R. R. Krchnavek, *IEEE Photon. Technol. Lett.* **1995**, 7, 535.
- [34] a) N. Sugiyama, in *Modern Fluoropolymers* (Ed: J. Scheirs), John Wiley & Sons, Chichester, UK **1997**, p. 541. b) Y. G. Zhao, W. K. Lu, Y. Ma, S. S. Kim, S. T. Ho, T. J. Marks, *Appl. Phys. Lett.* **2000**, 77, 2961.
- [35] P. R. Resnick, W. H. Buck, in *Modern Fluoropolymers* (Ed: J. Scheirs), John Wiley & Sons, Chichester, UK, **1997**, p. 397.
- [36] T. Watanabe, N. Ooba, S. Hayashida, T. Kurihara, S. Imamura, *J. Lightwave Technol.* **1998**, 16, 1049.
- [37] J. P. Kim, W. Y. Lee, J. W. Kang, S. K. Kwon, J. J. Kim, J. S. Lee, *Macromolecules* **2001**, 34, 7817.
- [38] C. Pitois, S. Vukmirovic, A. Hult, D. Wiesmann, M. Robertsson, *Macromolecules* **1999**, 32, 2903.
- [39] C. Pitois, D. Wiesmann, M. Lindgren, A. Hult, *Adv. Mater.* **2001**, 13, 1483.
- [40] *Polyimides* (Eds: D. Wilson, H. D. Stenzenberger, P. M. Hergenrother), Chapman and Hall, New York **1990**.
- [41] a) T. K. Kowalczyk, T. Kosci, K. D. Singer, A. J. Beuhler, D. A. Wargowski, *J. Appl. Phys.* **1994**, 76, 2505. b) R. Reuter, H. Franke, C. Feger, *Appl. Opt.* **1988**, 27, 4565.
- [42] S. K. Grayson, J. M. J. Fréchet, *Chem. Rev.* **2001**, 101(12), 3819.
- [43] J. M. Hagerhorst-Trewhella, J. D. Gelorme, B. Fan, A. Speth, D. Flagello, M. M. Oprysko, *Proc. SPIE-Int. Soc. Opt. Eng.* **1989**, 1177, 379.
- [44] a) J. H. Kim, E. J. Kim, H. C. Choi, C. W. Kim, J. H. Cho, Y. W. Lee, B. G. You, S. Y. Yi, H. J. Lee, K. Han, W. H. Jang, T. H. Rhee, J. W. Lee, S. J. Pearton, *Thin Solid Films* **1999**, 341, 192. b) K. Han, J. Kim, W. H. Jang, *J. Appl. Polym. Sci.* **2001**, 79, 176.
- [45] L. Eldada, *J. Lightwave Technol.* **1996**, 14, 1704.
- [46] a) D. Tomic, A. Mickelson, *Appl. Opt.* **1999**, 38, 3893. b) M. Jager, G. I. Stegeman, W. Brinker, S. Yilmaz, S. Mauer, W. H. G. Horsthuis, G. R. Mohlmann, *Appl. Phys. Lett.* **1996**, 68, 1183.
- [47] a) Y. Y. Maruo, S. Sasaki, T. Tamamura, *J. Lightwave Technol.* **1995**, 13, 1718. b) H. Nakayama, H. Fujimura, C. Egami, O. Sugihara, R. Matsushima, N. Okamoto, *Appl. Opt.* **1998**, 37, 1213. c) W. H. Wong, J. Zhou, E. Y. B. Pun, *Appl. Phys. Lett.* **2001**, 78, 2110.
- [48] D. Qin, Y. Xia, J. Rogers, R. Jackman, X. Zhao, G. M. Whitesides, in *Microsystem Technology in Chemistry and Life Sciences* (Eds: A. Manz, H. Becker), Vol. 194, Springer-Verlag, Berlin **1998**.
- [49] a) H. V. Shah, P. C. Deguzman, G. P. Nordin, J. M. Ballato, S. H. Foulger, D. W. Smith, Jr., *Polym. Mater. Sci. Eng.* **2000**, 83, 180. b) H. Shah, D. Smith, Jr., J. Ballato, S. Foulger, P. Deguzman, G. Nordin, *IEEE Photon. Technol. Lett.* **2000**, 12, 1650. c) B. T. Lee, M. S. Kwon, J. B. Yoon, S. Y. Shin, *IEEE Photon. Technol. Lett.* **2000**, 12, 62.
- [50] a) M. Hikita, R. Yoshimura, M. Usui, S. Tomaru, S. Imamura, *Thin Solid Films* **1998**, 331, 303. b) R. T. Chen, L. Wu, S. Tang, Y. S. Liu, C. Noddings, in *Sol-Gel and Polymer Photonic Devices* (Eds: M. P. Andrews, S. I. Najafi), Vol. CR 68, SPIE, Bellingham, MA **1997**, p. 228. c) J. Moisel, J. Guttman, H. P. Huber, O. Krumpoiz, M. Rode, R. Bogenberger, K. P. Kuhn, *Opt. Eng.* **2000**, 39, 673.
- [51] a) M. C. Oh, M. H. Lee, H. J. Lee, *IEEE Photon. Technol. Lett.* **1999**, 11, 1144. b) M. C. Oh, S. S. Lee, S. Y. Shin, W. Y. Hwang, J. J. Kim, *Electron. Lett.* **1996**, 32, 324.
- [52] E. Toussaere, N. Bouadma, J. Zyss, *Opt. Mater.* **1998**, 9, 255.
- [53] R. Yoshimura, H. Nakagome, T. Izawa, *Electron. Lett.* **1992**, 28, 2136.
- [54] a) C. L. Callender, J. F. Viens, J. P. Noad, L. Eldada, *Electron. Lett.* **1999**, 35, 1839. b) J. F. Viens, C. L. Callender, J. P. Noad, L. Eldada, *IEEE Photon. Technol. Lett.* **2000**, 12, 1010. c) Y. Hida, Y. Inoue, S. Imamura, *Electron. Lett.* **1994**, 30, 959. d) Y. H. Min, M. H. Lee, J. J. Ju, S. K. Park, J. Y. Do, *IEEE Sel. Top. Quantum Electron.* **2001**, 7, 806.
- [55] a) N. Keil, H. H. Yao, C. Zawadzki, *Appl. Phys. B* **2001**, 73, 619. b) N. Keil, H. H. Yao, C. Zawadzki, J. Bauer, M. Bauer, C. Dreyer, J. Schneider, *Electron. Lett.* **2001**, 37, 579.
- [56] T. A. Tumolillo, Jr., M. Donckers, W. H. G. Horsthuis, *IEEE Commun. Mag.* **1997**, February, 124.
- [57] a) N. Keil, H. H. Yao, C. Zawadzki, B. Strebel, *Electron. Lett.* **1994**, 30, 639. b) X. J. Lu, D. C. An, L. Sun, Q. J. Zhou, R. T. Chen, *Appl. Phys. Lett.* **2000**, 76, 2155.
- [58] a) N. Ooba, S. Toyoda, T. Kurihara, *Jpn. J. Appl. Phys.* **2000**, 39, 2369. b) U. Siebel, R. Hauße, K. Petermann, *IEEE Photon. Technol. Lett.* **2000**, 12, 40.
- [59] D. T. Chen, H. R. Fetterman, A. T. Chen, W. H. Steier, L. R. Dalton, W. S. Wang, Y. Q. Shi, *Appl. Phys. Lett.* **1997**, 70, 3335.
- [60] Y. Q. Shi, W. P. Lin, D. J. Olson, J. H. Bechtel, H. Zhang, W. H. Steier, C. Zhang, L. R. Dalton, *Appl. Phys. Lett.* **2000**, 77, 1.
- [61] A. T. Chen, V. Chuyanov, H. Zhang, S. Garner, S. S. Lee, W. H. Steier, J. H. Chen, F. Wang, J. S. Zhu, M. Q. He, Y. S. Ra, S. S. H. Mao, A. W. Harper, L. R. Dalton, H. R. Fetterman, *Opt. Eng.* **1999**, 38, 2000.
- [62] A. Domval, E. Toussaere, R. Hiehl, J. Zyss, *Synth. Met.* **2000**, 115, 21.
- [63] S. W. Ahn, S. Y. Shin, S. S. Lee, *Electron. Lett.* **2001**, 37, 172.
- [64] a) A. K.-Y. Jen, Y. Zhang, in *Photonic Polymer Systems* (Eds: D. L. Wise, G. E. Wnek, D. J. Trantolo, T. M. Cooper, J. D. Gresser), Marcel Dekker, New York **1998**, p. 847. b) M. H. Lee, Y. H. Min, J. J. Ju, J. Y. Do, S. K. Park, *IEEE J. Sel. Top. Quantum Electron.* **2001**, 7, 812.
- [65] S. Toyoda, A. Kaneko, N. Ooba, M. Hikita, H. Yamada, T. Kurihara, K. Okamoto, S. Imamura, *IEEE Photon. Technol. Lett.* **1999**, 11, 1141.
- [66] S. Toyoda, N. Ooba, T. Kitoh, T. Kurihara, T. Maruno, *Electron. Lett.* **2001**, 37, 1130.
- [67] S. S. Lee, J. U. Bu, S. Y. Lee, K. C. Song, C. G. Park, T. S. Kim, *IEEE Photon. Technol. Lett.* **2000**, 12, 407.
- [68] a) G. Karve, B. Bihari, R. T. Chen, *Appl. Phys. Lett.* **2000**, 77, 1253. b) D. An, Z. Yue, R. T. Chen, *Appl. Phys. Lett.* **1998**, 72, 2806.
- [69] L. H. Slooff, P. G. Kik, A. Tip, A. Polman, *J. Lightwave Technol.* **2001**, 19, 1740.
- [70] W. Huber, *Sens. Actuators, B* **1992**, 6, 122.
- [71] W. Lukosz, K. Tiefenthaler, *Sens. Actuators, B* **1988**, 15, 273.
- [72] R. G. Heidemann, *Sens. Actuators, B* **1993**, 10, 209.
- [73] D. Hah, E. Yoon, S. Hong, *Sens. Actuators, A* **2000**, 79, 204.
- [74] Y. Ren, P. Mormile, L. Petti, G. H. Cross, *Sens. Actuators, B* **2001**, 75, 76.
- [75] L. Eldada, S. Yin, C. Poga, C. Glass, R. Blomquist, R. A. Norwood, *IEEE Photon. Technol. Lett.* **1998**, 10, 1416.
- [76] L. Eldada, R. Blomquist, M. Maxfield, D. Pant, G. Boudoughian, C. Poga, R. A. Norwood, *IEEE Photon. Technol. Lett.* **1999**, 11, 448.
- [77] a) E. Yablonovitch, *Phys. Rev. Lett.* **1987**, 58, 2059. b) *Photonic Band Gap Materials* (Ed: C. M. Soukoulis), Kluwer, Dordrecht, The Netherlands **1996**.
- [78] J. P. Dowling, C. M. Bowden, *J. Mod. Opt.* **1994**, 41, 345.
- [79] H. Kosaka, T. Kawashima, A. Tomita, M. Notomi, T. Tamamura, T. Sato, S. Kawakami, *J. Lightwave Technol.* **1999**, 17, 2032.
- [80] R. T. Chen, B. Li, J. J. Foshee, W. B. Hartman, S. Tang, *Laser Focus World* **2000**, August, 139.
- [81] U. Siebel, R. Hauße, J. Bruns, K. Petermann, *IEEE Photon. Technol. Lett.* **2001**, 13, 957.
- [82] M. S. Yang, Y. O. Noh, Y. H. Won, W. Y. Hwang, *Electron. Lett.* **2001**, 37, 587.
- [83] a) C. Adachi, M. A. Baldo, S. R. Forrest, *Appl. Phys. Lett.* **2000**, 77, 904. b) S. R. Forrest, *IEEE J. Sel. Top. Quant. Electron.* **2000**, 6, 1072.
- [84] Y. Ohmori, M. Hikita, H. Kajii, T. Tsukagawa, K. Yoshino, M. Ozaki, A. Fujii, S. Tomaru, S. Imamura, H. Takenaka, J. Kobayashi, F. Yamamoto, *Thin Solid Films* **2001**, 393, 267.
- [85] S. Chandrasekhar, M. K. Hoppe, A. G. Dentai, C. H. Joyner, G. J. Qua, *IEEE Electron Device Lett.* **1991**, 12(10), 550.

- [86] D. C. Scott, D. P. Prakash, H. Erlig, D. Bhattacharya, M. E. Ali, H. R. Fetterman, *IEEE Microwave Guided Wave Lett.* **1998**, 8, 284.
- [87] L. Y. Lin, M. C. Wu, T. Itoh, T. A. Vang, R. E. Muller, D. L. Sivco, A. Y. Cho, *IEEE Trans. Microwave Theory Tech.* **1997**, 45, 1320.
- [88] S. M. Garner, S. S. Lee, V. Chuyanov, A. T. Chen, A. Yacoubian, W. H. Steier, L. R. Dalton, *IEEE J. Quantum. Electron.* **1999**, 35, 1146.
- [89] S. M. Garner, V. Chuyanov, S. S. Lee, A. T. Chen, W. H. Steier, L. R. Dalton, *IEEE Photon. Technol. Lett.*, **1999**, 11, 842.
- [90] a) N. Keil, H. H. Yao, C. Zawadzki, K. Losch, K. Satzke, W. Wischmann, J. V. Wirth, J. Schneider, J. Bauer, M. Bauer, *Appl. Phys. B* **2001**, 73, 49. b) N. Keil, H. H. Yao, C. Zawadzki, K. Losch, K. Satzke, W. Wischmann, J. V. Wirth, J. Schneider, J. Bauer, M. Bauer, *Electron. Lett.* **2001**, 37, 89.
- [91] T. A. Tumolillo, P. R. Ashley, *Proc. SPIE-Int. Soc. Opt. Eng.* **1993**, 2025, 507.
- [92] a) L. Friedrich, P. Dannberg, C. Wachter, T. Hennig, A. Brauer, W. Karthe, *Opt. Commun.* **1997**, 137, 239. b) B. Liu, A. Shakouri, P. Abraham, J. E. Bowers, *Electron. Lett.* **1999**, 35, 1552.
- [93] U. Streppel, P. Dannberg, C. Waechter, A. Braeuer, in *Design, Manufacturing, and Testing of Planar Optical Waveguide Devices* (Ed: R. A. Norwood), Vol. 4439, SPIE, Bellingham, MA **2001**, p. 72.
- [94] W. H. Steier, A. Chen, S. S. Lee, S. Garner, H. Zhang, V. Chuyanov, L. R. Dalton, F. Wang, A. S. Ren, C. Zhang, G. Todorova, A. Harper, H. R. Fetterman, D. T. Chen, A. Udapa, D. Bhattacharya, B. Tsap, *Chem. Phys.* **1999**, 245(1-3), 487.